

11-2008

Material selection and Optimization to Mitigate 316L Stainless Steel Corrosion in a Condensate Stabilizer

Afif Saif Nasser Harhara

Follow this and additional works at: https://scholarworks.uaeu.ac.ae/all_theses

Part of the [Materials Science and Engineering Commons](#)

Recommended Citation

Nasser Harhara, Afif Saif, "Material selection and Optimization to Mitigate 316L Stainless Steel Corrosion in a Condensate Stabilizer" (2008). *Theses*. 292.

https://scholarworks.uaeu.ac.ae/all_theses/292

This Thesis is brought to you for free and open access by the Electronic Theses and Dissertations at Scholarworks@UAEU. It has been accepted for inclusion in Theses by an authorized administrator of Scholarworks@UAEU. For more information, please contact fadl.musa@uaeu.ac.ae.



United Arab Emirates University
Deanship of Graduate Studies
Material Science and Engineering Program

**Material Selection and Optimization to Mitigate 316L
Stainless Steel Corrosion in a Condensate Stabilizer**

By

Afif Saif Nasser Harhara

A Thesis Submitted to United Arab Emirates University
in Partial Fulfillment of the Requirements
for the degree of Masters of Science in
Material Science and Engineering

Supervised By

Dr. Saud Aldajah

and

Dr. Ahmed Al-Awar

Mechanical Engineering Department
College of Engineering

November, 2008

Thesis Supervisors

Dr. Saud Aldajah

United Arab Emirates University
Mechanical Engineering Department
College of Engineering

and

Dr. Ahmed Al-Awar

United Arab Emirates University
Mechanical Engineering Department
College of Engineering

United Arab Emirates University
Graduate Studies
M.S.c. Program in Materials Science and Engineering

THESIS EXAMINATION REPORT

Student ID : 200350210
Student Name : Afif Saif Nasser Harhara
Title of the Thesis : Material Selection and Optimization to Mitigate 316 L Stainless Steel Corrosion in a Condensate Stabilizer

The Thesis Examination as A Partial Fulfillment of M. Sc. Degree in Materilas Science and Engineering Was conducted on Based on Examining the Thesis and the Students Presentation and the Subsequent Discussion, The Committee Recommends:

- Thesis is Satisfactory as is.
- Thesis is Satisfactory After Minor Modifications.
- Thesis should be Re-Evaluated After Major Modifications.
- Thesis is Rejected.

Examining Committee Members:

Thesis Supervisor: Name: <u>Saud Aldajah</u>	Signature: <u>[Signature]</u>	Date: <u>10/11/08</u>
Member: Name: <u>Abdenmour Seibi</u>	Signature: <u>[Signature]</u>	Date: <u>10-11-2008</u>
Member: Name: <u>Ahmad Alamar</u>	Signature: <u>[Signature]</u>	Date: <u>10-11-2008</u>
Member: Name: <u>Yousef Haik</u>	Signature: <u>[Signature]</u>	Date: <u>10-11-2008</u>
Member: Name:	Signature:	Date:

Approval of Program Coordinator:

Prof. [Signature] Date: 10-11-2008

APPROVAL:

Date :



Assistant Chief Academic Officer for Graduate Studies

Acknowledgment

Firstly, I want to express my gratitude to Allah, without his blessings; this effort would not have been achievable.

I am deeply indebted to my advisors, Dr. Saud Aldajah and Dr. Ahmed Al-Awar, for their constant support and valuable guidance. Their help and regular encouragement made this work possible.

I would also like to thank my colleagues at the masters program, my colleagues at work, and my friends. Their advice and patience are very much appreciated.

A special thanks also goes to Hasan Kamal who greatly contributed at helping me conduct the experimental work.

In addition, I must thank all of my managers at work for their support, and encouragement to complete this study.

Lastly, I take this opportunity to express my profound gratitude to my family: my parents, my wife and children (Fatima and Yousif), my brothers and sisters for all of their moral support and patience during my studies.

Table of Contents

Table of Contents.....	5
List of Figures.....	6
List of Tables.....	7
Summary.....	8
CHAPTER 1: Introduction.....	10
1.1 Petroleum Industry in the UAE.....	10
1.2 Corrosion Costs.....	11
1.3 Problem Definition.....	13
1.3.1 Inspection Findings.....	15
CHAPTER 2: Literature Review.....	22
2.1 Stainless Steels.....	22
2.1.1 Austenitic Stainless Steels.....	22
2.1.2 Martensitic Stainless Steels.....	24
2.1.3 Ferritic Stainless Steels.....	26
2.1.4 Precipitation Hardening Stainless Steels.....	28
2.1.5 Duplex Stainless Steels.....	31
2.2 Superalloys.....	32
2.2.1 Inconel 625.....	33
2.3 Corrosion of Stainless Steels.....	34
2.3.1 General Corrosion.....	35
2.3.2 Pitting Corrosion.....	35
2.3.3 Crevice Corrosion.....	36
2.3.4 Galvanic Corrosion.....	37
2.3.5 Intergranular Corrosion.....	39
2.3.6 Stress Corrosion Cracking.....	40
CHAPTER 3: Process Description.....	42
3.1 Gathering System and Inlet Facility.....	43
3.2 High Pressure Separation.....	45
3.3 Medium Pressure Separation.....	47
3.4 Condensate Stabilization.....	48
3.5 Storage and Shipping.....	52
CHAPTER 4: Experimental Study.....	53
4.1 Materials.....	53
4.1.1 U-Bends.....	54
4.2 Apparatus and Experimental Setup.....	56
4.3 Experimental Procedure.....	58
CHAPTER 5: Results and Discussion.....	59
5.1 Feed Analysis.....	59
5.2 Chemical Composition.....	60
5.3 Stress Calculation.....	61
5.4 Crack Initiation Tests.....	63
5.5 SEM Analysis.....	65
CHAPTER 6: Conclusions and Recommendations.....	71
References.....	73

List of Figures

Figure 1: A schematic diagram showing the upper part of the condensate stabilizer.....	14
Figure 2: severely corroded stainless steel 316L clip next to a new one	16
Figure 3: a schematic of the stainless steel clip and the branched cracking.....	16
Figure 4: Corroded stainless steel 316L clips with visual branched cracking.....	17
Figure 5: corroded stainless steel clip and its location inside condensate stabilizer	17
Figure 6: Corroded internals of stabilizer; stainless steel clips in location.....	18
Figure 7: Corrosion of the upper parts of the stabilizer column.	18
Figure 8: Internals of the bottom part of the stabilizer with no visual corrosion.....	19
Figure 9: Internals in the middle part of the condensate stabilizer	19
Figure 10: broken clips which fell from upper parts due to cracking	20
Figure 11: A block diagram of a condensate recovery plant.	43
Figure 12: Slug Catcher at the condensate recovery plant battery limit	45
Figure 13: Process Flow Diagram of the high pressure separator	46
Figure 14: A section of Piping and Instrumentation Diagram (PID) of HP separator.....	47
Figure 15: Process Flow Diagram of the medium pressure separator.	48
Figure 16: Condensate Stabilizer	49
Figure 17: PFD of overall stabilization section	51
Figure 18: Condensate stabilizer columns under construction	51
Figure 19: A schematic diagram of a condensate recovery	52
Figure 20: Method of bolting and stressing the U-Bends	55
Figure 21: Final U-Bend shape after stress is applied	55
Figure 22: U-Bend specimens of stainless steel 316L and inconel 625	55
Figure 23: Assembled apparatus as per ASTM G-36	57
Figure 24: Assembled apparatus with a close up of water condenser and trap	57
Figure 25: A three week temperature trend of the top part of the condensate stabilizer ..	59
Figure 26: Geometry of a U-Bend specimen	62
Figure 27: Crack initiation time for stainless steel 316L U-Bend specimen in solution ..	64
Figure 28: Crack initiation time for inconel U-Bend specimen in solution.....	64
Figure 29: Macrograph of the surface of stainless steel 316L (Resolution 1000).....	66
Figure 30: Macrograph of the surface of inconel 625 (Resolution 1000).....	66
Figure 31: Macrograph of the crack of controlled stainless steel 316L (Resolution 35)..	67
Figure 32: Macrograph of the crack of controlled inconel 625 (Resolution 35)	67
Figure 33: Macrograph of the crack of controlled stainless steel 316L (Resolution 50)..	68
Figure 34: Macrograph of the crack of controlled inconel 625 (Resolution 50)	68
Figure 35: Macrograph of original crack of stainless steel 316L clip (Resolution 35)	69
Figure 36: Macrograph of original crack of stainless steel 316L clip (Resolution 50)	69

List of Tables

Table 1: Feed constituents to the condensate recovery plant.....	21
Table 2: Operating parameters of condensate stabilizer.....	21
Table 3: Design parameters of high pressure separator.....	46
Table 4: Design parameters of medium pressure separator.....	48
Table 5: Design parameters of condensate stabilizers.....	50
Table 6: Material specification of stainless steel 316L and inconel 625.....	54
Table 7: Chloride content in water samples from draw off drums of both stabilizers.....	59
Table 8: Chemical composition of original stainless steel 316L clip.....	60
Table 9: Chemical composition of purchased stainless steel 316L sample.....	60
Table 10: Chemical composition of inconel 625 sample.....	61
Table 11: Dimensions of U-Bend specimens (average of 6 specimen).....	62
Table 12: Dimension of inconel U-Bend specimens (average of 6 specimens).....	63
Table 13: Crack initiation time for specimen in boiling magnesium chloride solution....	64

List of Tables

Table 1: Feed constituents to the condensate recovery plant.....	21
Table 2: Operating parameters of condensate stabilizer	21
Table 3: Design parameters of high pressure separator	46
Table 4: Design parameters of medium pressure separator	48
Table 5: Design parameters of condensate stabilizers	50
Table 6: Material specification of stainless steel 316L and inconel 625	54
Table 7: Chloride content in water samples from draw off drums of both stabilizers.....	59
Table 8: Chemical composition of original stainless steel 316L clip	60
Table 9: Chemical composition of purchased stainless steel 316L sample	60
Table 10: Chemical composition of inconel 625 sample.....	61
Table 11: Dimensions of U-Bend specimens (average of 6 specimen).....	62
Table 12: Dimension of inconel U-Bend specimens (average of 6 specimens)	63
Table 13: Crack initiation time for specimen in boiling magnesium chloride solution....	64

Summary

The United Arab Emirates (UAE) is one of the key players of the oil and gas industry of the world; with oil reserves estimated at 9% of the total world reserves, the petroleum industry is considered to be the backbone of the economy.

In one of the gas processing facilities in Abu Dhabi, UAE; a case of material failure occurred in the fractionating column twice in a cycle of less than 2 years. The material used for the internals of the column was stainless steel 316L. The different types of stainless steel corrosion were studied with emphasis on the suspected stress corrosion cracking; superalloys were also studied as an alternative material, especially nickel based superalloys.

The material failure was investigated in relation to the type of failure, and all the operating conditions associated to the corroded part of the column were studied and identified. Several tests were conducted to analyze the feed and the product of the column, as well as the presence of chlorides in the zones that suffered mostly of severe corrosion.

In an effort to conduct accelerated stress corrosion cracking tests, all tests were carried out according to ASTM G36 standard, which does not replicate the exact field conditions, but provides us with guidelines in which the material possesses better stress corrosion resistivity.

The experimental work included testing the stainless steel 316L in an accelerated corrosion environment, and comparing the results with a proposed higher corrosion resistant nickel alloy (Inconel). According to ASTM G36 standard; the boiling magnesium chloride provided the accelerated corrosion environment, and the test materials were shaped into U-Bend specimens as they undergo both plastic and elastic stresses. The specimens were then tested to determine the time required for cracks to initiate. The cracked specimens were prepared for Scanning Electron Microscope examination.

The results of the experimental work showed that the main mode of failure was stress corrosion cracking initiated by the proven presence of chlorides, hydrogen sulfide and water at elevated temperatures. Inconel 625 samples in controlled environment showed better corrosion resistance as it took an average of 56 days to initiate cracks, whereas it took an average of 24 days to initiate cracks in stainless steel 316L samples. The SEM macrographs showed that the cracks in the stainless steel 316L samples were longer, wider, and deeper compared to the cracks of inconel 625.

CHAPTER 1: Introduction

1.1 Petroleum Industry in the UAE

The United Arab Emirates (UAE) is considered one of major oil and gas producers in the world. It is a member of the Organization of the Petroleum Exporting Countries (OPEC) and of the Organization of Arab Petroleum Exporting Countries (OAPEC). The UAE has an estimated oil reserves of 97.8 billion barrels; ranked 5th of the world. The emirate of Abu Dhabi alone accounts for around 92.2 billion barrels of reserves, UAE has 9.6% of the worlds total oil reserves. ¹

The majority of the UAE's crude oil is considered light, with gravities in the 32° to 44° API range. Abu Dhabi's Murban 39° blend is the UAE's primary export crude. Proven oil reserves in Abu Dhabi have roughly doubled in the last decade, mainly due to the significant increase in the rates of recovery. Abu Dhabi has continued to identify new oil wells, especially offshore, and to discover new oil-rich structures in existing fields.

Natural gas reserves of the UAE are also high estimated at 213.5 trillion cubic feet; ranked 4th of the world with respect to natural gas reservoirs. Current natural gas reserves are projected to last for about 150-170 years.² Increased domestic consumption of electricity and growing demand on the petrochemical industry provided incentives for the UAE to increase its use of natural gas. Over the last decade, natural gas consumption in Abu Dhabi has doubled, and it currently stands at nearly 4 billion cubic feet per day. The

development of natural gas fields also resulted in increased production and exports of condensates, which are not subject to OPEC production quotas.³

The statistics indicate that the UAE currently has one of the fastest growing economies in the world. According to a recent report by the Ministry of Finance and Industry, real Gross Domestic Product (GDP) rose by 35 percent in 2006 to \$175 billion, compared with \$130 billion in 2005. These figures would suggest that the UAE had the fastest growing real GDP in the world, between 2005 and 2006.⁴

Although the United Arab Emirates is becoming less dependent on natural resources as a source of revenue, petroleum and natural gas exports still play an important role in the economy, especially in Abu Dhabi.⁵ The gas and oil industry is still the basic and most important of the UAE's industries. This is why multi-billion dollar projects are still being implemented and awarded in the oil and gas sector, in order to increase the production capacities of the oil fields, increase the handling capacities of refineries, build new ones, and handle the additional associated gas, along with the non-associated gas and sour gas. Recently a 5 billion dollar project was awarded to utilize the sour gas associated to one of the remote gas fields.⁶

1.2 Corrosion Costs

According to a study conducted by the United States Federal Highway Administration on the direct costs associated with metallic corrosion in the U.S. estimated that the total annual direct cost of corrosion in the U.S. is a staggering \$276 billion (approximately

3.1% of GDP of the US). The study entitled "Corrosion costs and Preventive Strategies in the United States" was conducted from 1999 to 2001 by CC Technologies Laboratories, Inc., with support from the FHWA and NACE. Its main activities included determining the cost of corrosion control methods and services, determining the economic impact of corrosion for specific industry sectors, and extrapolating individual sector costs to a national total corrosion cost.⁷

Corrosion costs in the petroleum industry in general, and in UAE's petroleum industry in particular compromises of corrosion monitoring and prevention. Corrosion inhibitors are used along with other chemicals to manipulate conditions such as pH controllers and oxygen scavengers. Corrosion monitoring such as online corrosion probes, and corrosion coupons are also applied in various suspected locations in the plants. The periodic inspection, online and under scheduled shutdowns also contributes to the costs associated with corrosion.

On the other hand, corrosion allowances in design, which vary from 20% to sometimes over 300% according to the service and the severity of the equipment, vessel, or pipeline. High percentages of allowances are considered justifiable where damages could be classified as catastrophic or damaging to life or environment; these allowances are added as safety margins to compensate for the corrosion losses.

Coating of internals and externals is also used to protect against corrosion, as well as other means implemented such as cathodic protection (both induced current and

sacrificial anode). Cathodic protection of all pipelines, vessels, and even well head facilities is mandatory in the UAE.

1.3 Problem Definition

Condensate stabilizers are fractionation-type stabilizing columns used in the petrochemical industry. The main purpose of the column is to remove light fractions of hydrocarbons to maintain a desired Reid Vapor Pressure (RVP) and remove H₂S content of the gas. They are similar in principal with any fractionating tower where heat and material exchange takes place, and components stay in partial equilibrium in each stage or tray. This fractionation gives either multiple products from individual trays, or main products from top and bottom trays.

In this case, the inlet of the stabilizer is sour gas which is routed to the stabilizer after gravity separation at different pressures (flashing), and the product is condensate, which is defined as hydrocarbon liquid associated with gas, Pentane and heavier Hydrocarbons (C₅+).

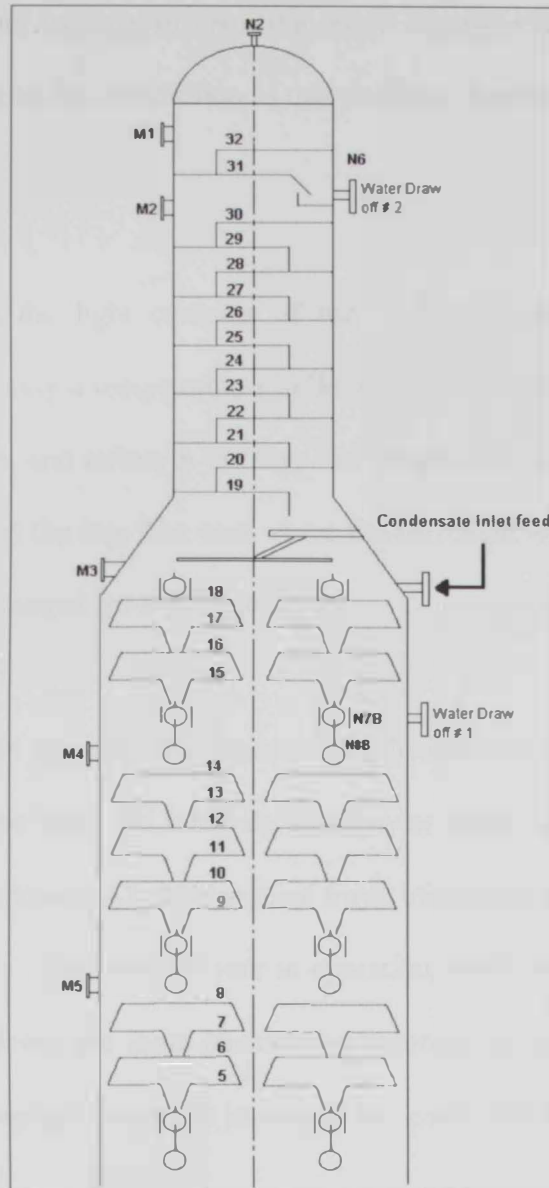


Figure 1: A schematic diagram showing the upper part of the condensate stabilizer

A standard stabilizer column contains 32 stainless steel trays, and it is equipped with two bottom re-boilers, and two side re-boilers. It is also equipped with two water draw-off drums to remove any water that was carried over from previous separation processes.

Figure 1 shows a schematic diagram of the stabilizer column.

One frequent problem in such stabilizers is the severe corrosion of the stainless steel trays in the upper part of the tower. In addition to this problem, cracking of tray clips and bolts is widespread.

The column removes the light contents of the feed gas and stabilizes the product condensate by maintaining a temperature profile in the entire tower; this is done via the re-boiler in the bottom, and reflux in the top. The temperature profile starts at 200°C in the bottom, and 50°C at the top. The area where the corrosion was widely spread (upper part) the temperatures ranged from 90°C to 50°C.

The stabilizer column in the study here underwent scheduled maintenance shutdown after being in service for one year; the internals which were made of stainless steel 316L at certain locations in the tower. All the damaged trays, clips were replaced and the column was put back in service. After another year in operation, when the column was inspected in the scheduled shutdown, the same phenomena occurred again in the same part of the column. The next paragraph describes in details the corrosion areas and the inspection findings.

1.3.1 Inspection Findings

The inspection report of the condensate stabilizer stated that severe general corrosion was found in the higher stainless steel trays (Trays 19 and above) whereas the lower trays experienced less corrosion. All the stainless steel clips in the higher trays were also severely corroded; 60% of these severely corroded clips fell from their location the column. The stainless steel clips cracking was observed to be branched type, this

phenomena took place in the same exact location of all clips. The cracking location observed to be cold worked in fabrication (residual stress) as well as subjected to bolt tensioning (applied stress). The following figures show the corrosion of stainless steel 316L clips of the condensate stabilizer and the stabilizer internals:



Figure 2: Severely corroded stainless steel 316L clip next to a new one

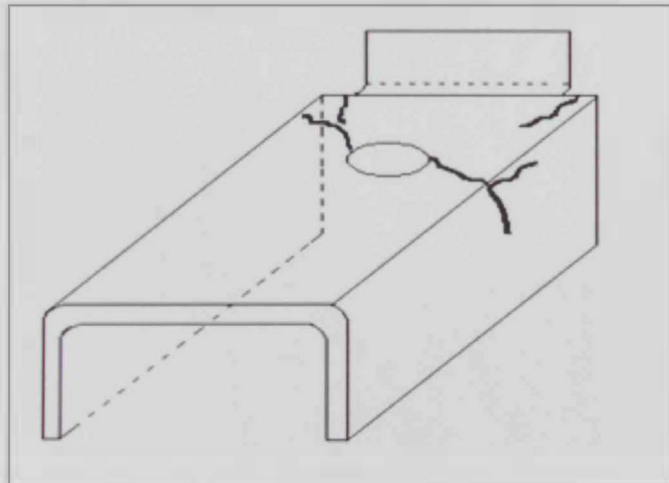


Figure 3: A schematic of the stainless steel clip and the branched cracking

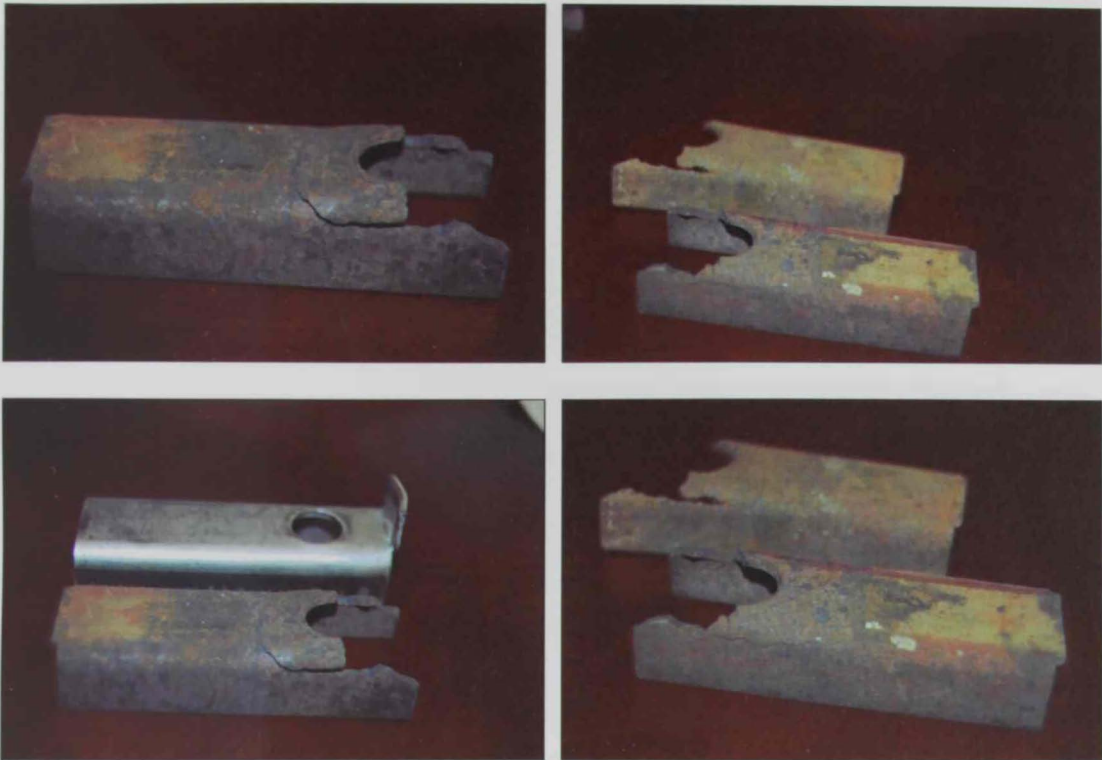


Figure 4: Corroded stainless steel 316L clips with visual branched cracking.



Figure 5: Corroded stainless steel clip and its location inside condensate stabilizer

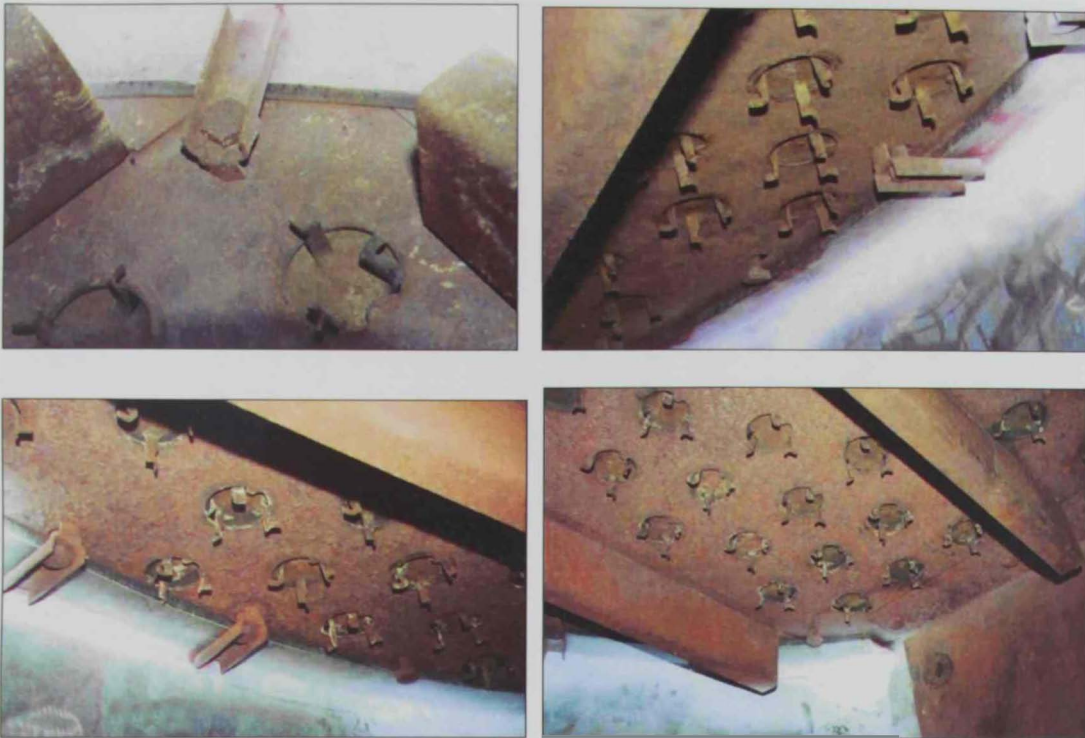


Figure 6: Corroded internals of stabilizer; stainless steel clips in location

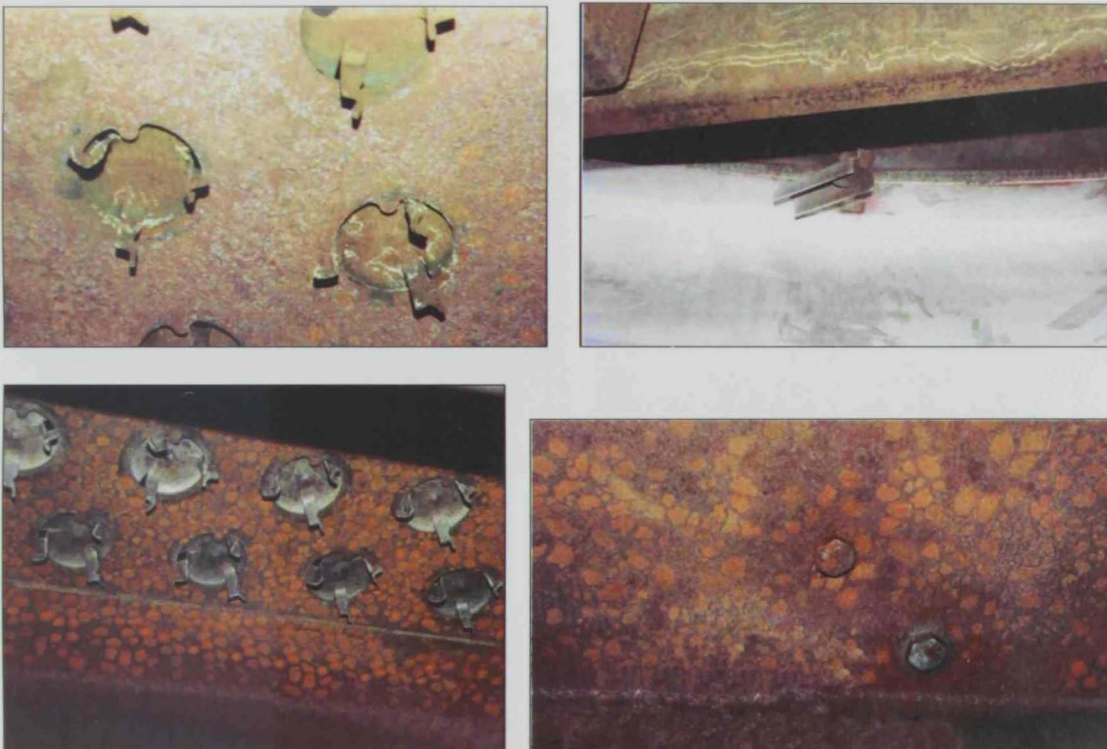


Figure 7: Corrosion of the upper parts of the stabilizer column.

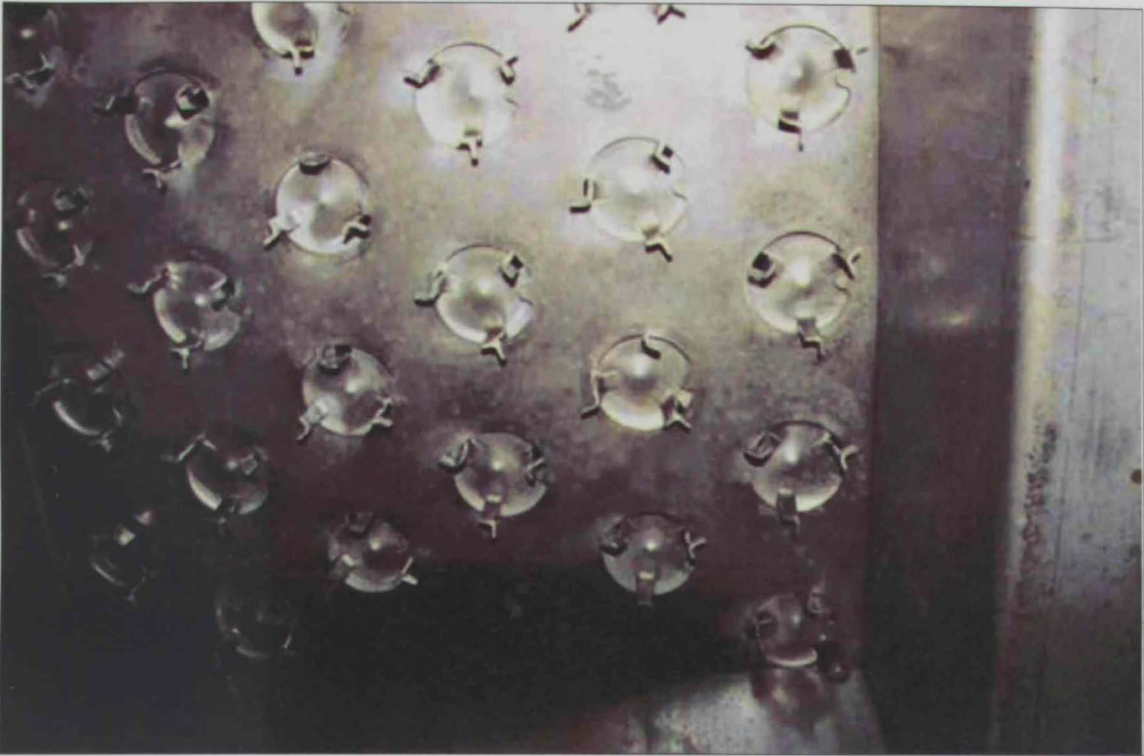


Figure 8: Internals of the bottom part of the stabilizer with no visual corrosion

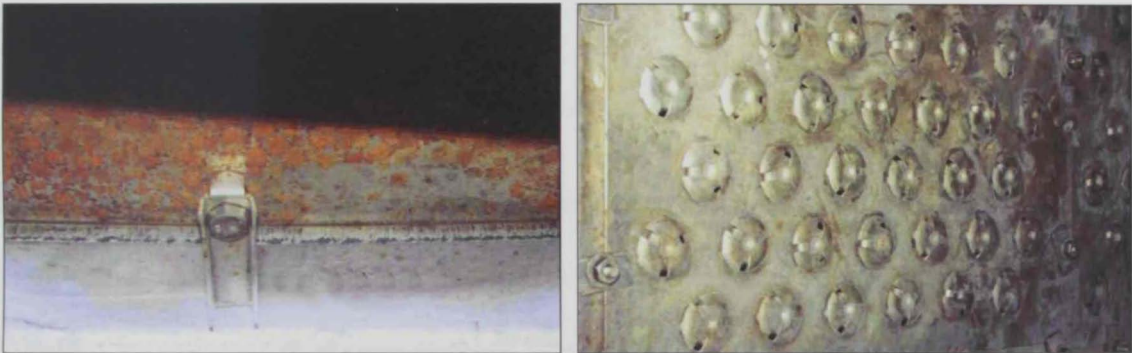


Figure 9: Internals in the middle part of the condensate stabilizer



Figure 10: Broken clips which fell from upper trays due to cracking

Gas chromatography was carried out for the feed to the stabilizer column, as it was suspected that the main reason for the failure of the tower internals was the presence of chlorides with high concentrations.

The following table shows components of the feed gas to the stabilizer column. Although no chlorides were observed in the test, yet it is assumed that always low concentrations of chlorides sometimes are present ranging from 0 to 1000PPM, this is believed to happen while opening of new wells, or increasing or reducing the chokes (feed), as these operations increases the amounts of sour water that is introduced to the column, and disturbs the equilibrium inside the column.

Component	Mole %	Component	Mole %	Component	Mole %	Component	Mole %
H ₂ O	1.88	iC5	0.84	nC13	0.26	CS ₂	0.000027
N ₂	0.29	nC5	0.99	nC14	0.19	CH ₄ S	0.0025
CO ₂	4.07	nC6	1.33	nC15	0.12	ETSH	0.00067
H ₂ S	2.46	nC7	1.33	nC16	0.09	N-Propyl Mercaptan	0.00034
C1	69.41	nC8	1.29	nC17	0.07	N-Butyl Mercaptan	0.00022
C2	6.4	nC9	1.03	nC18	0.05	Dimethyl Sulfide	0.000005
C3	3.49	nC10	0.76	nC19	0.04	Dimethyl Disulfide	0.000007
iC4	0.88	nC11	0.47	nC20	0.12	Pentyl Mercaptan	0.0027
nC4	1.82	nC12	0.32	COS	0.0028	TOTAL	100

Table 1: Feed constituents to the condensate recovery plant

The chloride content in the feed and product of the stabilizer were repeated several times, with changing the operating conditions, and feed conditions. The results of these tests were inconclusive of presence of high chloride content (above 1000 PPM). The investigations suggested that this type of corrosion might be stress corrosion cracking.

The stabilizer column internals were replaced again, and it was put back to service. The following table shows the operating conditions of the stabilizer column. Design parameters and process description of the condensate stabilizer is elaborated in the literature review. Table 2 lists some of the operating parameters of the stabilizer:

Parameter	Operating Condition
Temperature (Bottom)	200°C
Temperature (Top)	50°C
Pressure	12 Bar
pH	5
RVP	8 psia

Table 2: Operating parameters of condensate stabilizer

CHAPTER 2: Literature Review

2.1 Stainless Steels

Stainless steel is an iron-carbon alloy with chromium as the predominant alloying element. Iron does not occur in its native state because it combines with oxygen and other elements. It is extracted from its ore and if given the opportunity, tends to revert to a compound by reacting with the environment. Rusting is an example of this reversion process. The process can be retarded by adding chromium, which at sufficiently large concentrations forms a protective oxide film at the surface. The nature of this oxide film depends on the chromium concentration, a passive film of chromium oxide only about 1-2 nm thick covers the steel, which becomes stainless as long as the chromium is in solid solution in the steel.⁸ A minimum chromium concentration of 11 wt% is required. Stainless steels are highly resistant to corrosion in a variety of environments, and the corrosion resistance can be further enhanced by nickel and molybdenum additions.⁹

Stainless steels are also classified by their crystalline structure to the following 5 types:

2.1.1 Austenitic Stainless Steels

Austenitic stainless steels: (200-300 series) are generally composed of chromium, nickel and manganese in iron. They contain a maximum of 0.15% carbon, a minimum of 16% chromium and sufficient nickel and/or manganese to retain an austenitic structure at all temperatures from the cryogenic region to the melting point of the alloy.¹⁰

Characteristics

Carbon steel when cooled transforms from Austenite to a mixture of ferrite and cementite; whereas with austenitic stainless steel, the high chrome and nickel content suppress this transformation keeping the material fully austenite on cooling (The Nickel maintains the austenite phase on cooling and the Chrome slows the transformation down so that a fully austenitic structure can be achieved with only 8% Nickel).

Austenitic stainless steels are hardened by cold working; they are the most ductile of all stainless steels and hence can be formed easily.¹¹ Austenitic stainless steels also have low yield stress and relatively high ultimate tensile strength. Austenitic steels have a face centered cubic atomic structure which provides more planes for the flow of dislocations, giving this type of steels its good ductility. Heat treatment and the thermal cycle caused by welding, have little influence on mechanical properties. However strength and hardness can be increased by cold working, which will also reduce ductility.

Corrosion Resistance

High corrosion resistance of austenitic stainless steels is primarily attributed to the passive oxide film formed on its surface that, exposed to an aqueous solution, is a mixture of iron and chromium oxides, with hydroxide and water-containing compounds located in the outermost region of the film, and chromium oxide enrichment at the metal-film interface. However, the resistance of this passive film is determined by the environmental conditions which the stainless steel is exposed to, as well as by the alloy composition.¹²

Austenitic stainless steels generally have good corrosion resistance, but quite severe corrosion can occur in certain environments. They are highly susceptible to stress corrosion cracking. Probably the biggest cause of failure in pressurized plants made of stainless steel is stress corrosion cracking. This type of corrosion forms deep cracks in the steel and is caused by the presence of chlorides in the process fluid, elevated temperatures and the steel is subjected to tensile stresses.¹³

Applications

Austenitic stainless steels are the most widely used in and comprise 70% of the total production of stainless steels in the world; these steels are used in a variety of applications such as welded construction, fittings, heat exchangers, furnaces, and components for severe chemical environments.

2.1.2 Martensitic Stainless Steels

Martensitic stainless steels are similar to low alloy or carbon steels, having a structure similar to the ferritic steels. They are capable of being heat treated in such a way that martensite is the prime micro-constituent. Addition of alloying elements in significant concentrations produces dramatic alterations in the iron-iron carbide phase diagram. However, due the addition of carbon, they can be hardened and strengthened by heat treatment, in a similar way to carbon steels. The main alloying element is chromium, typically (12-14%), molybdenum (0.2-1%), nickel (0-2%), and carbon (0.1-1%).¹⁴

Characteristics

Martensitic stainless steels Body Centered Tetragonal (BCT). They are classified as a hard ferro-magnetic group. In the annealed condition, they have low tensile yield strengths which make them capable of being machined and cold worked. The strength obtained by heat treatment depends on the carbon content of the alloy; increasing the carbon content increases the strength and hardness potential but decreases ductility and toughness.

Corrosion Resistance

Martensitic stainless steels are not as corrosion resistant as the other two classes but they are extremely strong, tough, and highly machinable. In comparison with the austenitic and ferritic grades of stainless steels, martensitic stainless steels are less resistant to corrosion, although they can be developed with nitrogen and nickel additions to improve corrosion resistance but with lower carbon levels than the traditional grades.

Weldability of martensitic stainless steels has always been a concern owing to the cracking problems in the weld metal and heat affected zones. Investigations has brought out the fact that thin sections of Martinsitic stainless steels such as the AISI 410 can be welded in the annealed condition without the problem of cracking; with weldments showing matching mechanical properties and microstructural variations not influencing the general corrosion and passivation behavior.¹⁵

Applications

Martensitic stainless steels are suitable for applications where the material is subjected to both corrosion and wear. Typical applications include aerospace, automotive, electric

engines, cutlery, power hand tools, pump parts, valve seats, ball bearings, and surgical instruments.

2.1.3 Ferritic Stainless Steels

Ferritic steels (400 series) have a high chromium content. They are magnetic and have high corrosion resistance, but have lower ductility than austenitic stainless steels. They contain between 10.5% and 27% chromium and very little nickel, but some types can contain lead, molybdenum, aluminum or some titanium. Ferritic stainless steels have certain useful corrosion properties, such as resistance to chloride stress-corrosion cracking, corrosion in oxidizing aqueous media, oxidation at high temperatures and pitting and crevice corrosion in chloride media.

Characteristics

Ferritic stainless steels are hardened by cold working and they are not heat treatable. Structures of these steels are kept completely ferritic at room and high temperature by adding titanium or columbium, or by melting to very low levels of carbon and nitrogen, or both. Such microstructures provide ductility and corrosion resistance. Molybdenum improves pitting corrosion resistance, while silicon and aluminum increase resistance to high temperature oxidation.¹⁶

Corrosion Resistance

Resistance to stress-corrosion cracking is the most obvious advantage of the ferritic stainless steels. Ferritic steels resist chloride and caustic stress corrosion cracking very well. Nickel and copper residuals lower resistance of these steels to stress corrosion.

Susceptibility of the ferritic steels to intergranular corrosion is due to chromium depletion, caused by precipitation of chromium carbides and nitrides at grain boundaries. Because of the lower solubility for carbon and nitrogen and higher diffusion rates in ferrite, the synthesized zones of welds in ferritic steels are in the weld and adjacent to the weld. To eliminate the intergranular corrosion, it is necessary either to reduce carbon to very low levels, or to add titanium and columbium to tie up the carbon and nitrogen.

High-chromium ferritic steels have 18-30% Cr and low content of carbon and nitrogen. Titanium in these alloys prevents intergranular chromium-carbide and nitride precipitation during welding or processing. Because of the ferritic structure and controlled composition, the alloys exhibit good resistance to general, intergranular and pitting corrosion, and stress corrosion cracking. Similar to other high chromium stainless steels, types 442 and 446 have excellent oxidation resistance at elevated temperatures. They also have high thermal conductivity, higher yield strength than austenitic stainless steels, and lower tensile ductility.¹⁷

The excellent resistance to chlorides, organic acids and chloride stress-corrosion indicates that these alloys should be suitable for a wide range of applications in which conventional stainless steels or other materials are either inadequate or uneconomical. High-chromium ferritic stainless steels are useful in heat exchanger tubing, feed-water tubing and in equipment that operate with chloride-bearing or brackish cooling waters.

Applications

Ferritic stainless steels were generally used for nonstructural applications, such as kitchen equipment and automotive accessories; but after the development of high chromium ferritic steels, they are finding substantial applications in replacing brass and cupronickel, corrosion-resistant high-nickel alloys, and other materials in the food processing, power, chemical, petrochemical, marine and pulp and paper industries.

2.1.4 Precipitation Hardening Stainless Steels

Precipitation-hardening martensitic stainless steels have corrosion resistance comparable to austenitic varieties, but can be precipitation hardened to even higher strengths than the other martensitic grades. The most common, 17-4PH, uses about 17% chromium and 4% nickel.

Precipitation hardening stainless steels are chromium and nickel containing steels that provide an optimum combination of the properties of martensitic and austenitic grades. Like martensitic grades, they are known for their ability to gain high strength through heat treatment and they also have the corrosion resistance of austenitic stainless steels.

The high tensile strengths of precipitation hardening stainless steels come after a heat treatment process that leads to precipitation hardening of a martensitic or austenitic matrix. Hardening is achieved through the addition of one or more of the elements Copper, Aluminium, Titanium, Niobium, and Molybdenum.

The most well known precipitation hardening steel is 17-4 PH. The name comes from the additions 17% Chromium and 4% Nickel. It also contains 4% Copper and 0.3% Niobium. 17-4 PH is also known as stainless steels grade 630.¹⁸ 17-4 PH stainless steel has been called the workhorse of PH stainless steels by virtue of its high strength, excellent corrosion resistance and relatively simple heat treatment. However, the wider applications are restricted by their relatively low hardness and poor mechanical properties. Therefore, they cannot meet challenging design requirements of high strength, high toughness and good resistance to both corrosion and wear in some applications such as turbine blades, tools, bearings and even orthopedic surgery.¹⁹

The advantage of precipitation hardening steels is that they can be supplied in a solution treated condition, which is readily machine able. After machining or another fabrication method, a single, low temperature heat treatment can be applied to increase the strength of the steel; this is known as ageing or age hardening, as it is carried out at low temperature, the component undergoes no distortion.

Characteristics

Precipitation hardening stainless steels are characterized into one of three groups based on their final microstructures after heat treatment. The three types are: martensitic (17-4 PH), semi-austenitic (17-7 PH) and austenitic (A-286).

Martensitic Alloys: Martensitic precipitation hardening stainless steels have a predominantly austenitic structure at annealing temperatures of around 1040 to 1065°C.

Upon cooling to room temperature, they undergo a transformation that changes the austenite to martensite.

Semi-austenitic Alloys: Unlike martensitic precipitation hardening steels, annealed semi-austenitic precipitation hardening steels are soft enough to be cold worked. Semi-austenitic steels retain their austenitic structure at room temperature but will form martensite at very low temperatures.

Austenitic Alloys: Austenitic precipitation hardening steels retain their austenitic structure after annealing and hardening by ageing. At the annealing temperature of 1095 to 1120°C the precipitation hardening phase is soluble. It remains in solution during rapid cooling. When reheated to 650 to 760°C, precipitation occurs. This increases the hardness and strength of the material. Hardness remains lower than that for martensitic or semi-austenitic precipitation hardening steels austenitic alloys remain nonmagnetic.

Corrosion Resistance

Precipitation hardening stainless steels have moderate to good corrosion resistance in a range of environments. They have a better combination of strength and corrosion resistance than when compared with the heat treatable 400 series martensitic alloys. Corrosion resistance is similar to that found in grade 304 stainless steels. In warm chloride environments, 17-4 PH is susceptible to pitting and crevice corrosion. When aged at 550°C or higher, 17-4 PH is highly resistant to stress corrosion cracking. Better stress corrosion cracking resistance comes with higher ageing temperatures. Corrosion

resistance is low in the solution treated (annealed) condition and it should not be used before heat treatment.

Applications

Due to the high strength of precipitation hardening stainless steels, most applications are in aerospace and other high-technology industries. Some of the other applications include gears, valves, engine components, high strength shafts, turbine blades, and molding dies.

2.1.5 Duplex Stainless Steels

Duplex stainless steels have a mixed microstructure of austenite and ferrite, the aim being to produce a 50/50 mix, although in commercial alloys, the mix may be 40/60 respectively. Duplex steels have improved strength over austenitic stainless steels and also improved resistance to localized corrosion, particularly pitting, crevice corrosion and stress corrosion cracking.

Characteristics

They are characterized by high chromium (19–28%) and molybdenum (up to 5%) and lower nickel contents than austenitic stainless steels. Duplex stainless steels are mostly used in petrochemical industry.²⁰

Corrosion Resistance

The high corrosion resistance and the excellent mechanical properties combination of duplex stainless steels can be explained by their chemical composition and balanced

microstructure of approximately equivalent volume fractions of ferrite and austenite. Firstly, the chemical composition based on high contents of Cr improves inter-granular resistance, and Mo improves the resistance to pitting corrosion. Moreover, additions of nitrogen can promote structural hardening by interstitial solid solution mechanism, which raises the yield strength and ultimate strength values without impairing toughness. Secondly, the two-phase microstructure guarantees higher resistance to pitting and stress corrosion cracking in comparison with conventional stainless steels. Duplex stainless steels are suitable for many marine and petrochemical applications because of their good resistance to pitting and stress corrosion cracking. Since they are used in very aggressive environment containing high chloride concentration at high temperature, their performance, particularly localized corrosion resistance, becomes a major concern to material scientists and processing engineers.²¹

2.2.1 Inconel 625

Applications

Typical applications of duplex stainless steels include oil and gas exploration, paper and pulp processing, chemical processing applications, and other high chloride environments. It is also used in marine and offshore structures, as they require special materials due to the highly corrosive environments in which they exist.

2.2 Superalloys

A superalloy is defined as an alloy that exhibits excellent mechanical strength and creep resistance at high temperatures, good surface stability, and corrosion and oxidation resistance. Superalloys typically have an austenitic face centered cubic crystal structure.

Superalloys were developed since the second quarter of the 20th century as materials for elevated temperature applications and can be divided in three groups: nickel-base superalloys, cobalt-base superalloys and iron base superalloys²². Many of the industrial nickel-based superalloys contain alloying elements including chromium, aluminum, and titanium. They also contain other alloying elements in smaller percentages such as molybdenum, tungsten, niobium, tantalum and cobalt.

Superalloys are used where there is a need for high temperature strength and corrosion/oxidation resistance; typical applications are in the aerospace industry (aircrafts, jet engines, rocket engines, and space vehicles), petroleum industry (gas turbine blades, impellers, chemical processing vessels, and heat exchanger tubing), submarines, nuclear power plants and reactors.

Examples of superalloys are Hastelloy, Inconel, Rene and Monel.²³

2.2.1 Inconel 625

Inconel-625 is a non-magnetic, corrosion and oxidation-resistant, nickel-base alloy. Its outstanding strength and toughness in the temperature range cryogenic to 1093 °C are derived primarily from the solid solution strengthening effects of the refractory metals, niobium and molybdenum, in a nickel–chromium matrix. Nickel and chromium provide resistance to oxidizing environment, while nickel and molybdenum to non-oxidizing environment.²⁴ Pitting and crevice corrosion are prevented by molybdenum. Niobium stabilizes the alloy against sensitization during welding. Its resistance to chloride stress-corrosion cracking is excellent. It also resists scaling and oxidation at high temperatures. Some typical applications for Inconel-625 are heat shields, furnace hardware, gas turbine

engine ducting, combustion liners and spray bars, chemical plant hardware and special seawater applications.²⁵

Nickel base superalloy, Inconel 625 is widely used in aeronautical, aerospace, chemical, petrochemical and marine applications. The choice for this material is based upon a good combination of yield strength, tensile strength, creep strength, excellent fabricability, weldability and good resistance to high temperature corrosion on prolonged exposure to aggressive environments.²⁶ Although the alloy was initially designed to be used in solid solution strengthened condition, it is observed that precipitation of inter-metallic phases and carbides occurs on subjecting the alloy to ageing treatment.²⁷

2.3 Corrosion of Stainless Steels

Although corrosion resistance is one of the main reasons why stainless steels are used, yet they do in fact suffer from certain types of corrosion. The misconception of stainless steels that they are not affected by corrosion largely comes from the phenomenal change it got to the industry since they were developed in the early 1900's.

In some environments care must be taken to select correct grade of stainless steel which will be suitable for the application; as the basic resistance of stainless steel occurs because of its ability to form a protective coating on the metal surface. This coating is a passive film which resists further oxidation or rusting. The formation of this film is instantaneous in an oxidizing atmosphere such as air, water, or other fluids that contain

oxygen. Once the layer has formed, it is said that the metal is passivated, and the oxidation (rusting) rate will slow down.²⁸

The passive film is invisible in stainless steels where it is clearly visible in aluminum or silver. It is created when oxygen combines with chrome to form chrome oxide which is more commonly called ceramic. This protective oxide or ceramic coating is common to most corrosion resistant materials. Halogen salts, especially chlorides easily penetrate this passive film and will allow corrosive attack to occur.

The corrosion of stainless steel could be categorized to the following types:

2.3.1 General Corrosion

It is a uniform type of corrosion that affects the passive film formed on the stainless steel. It affects the entire surface of the metal and shows a uniform sponge like appearance. The rate of attack is affected by the fluid concentration, temperature, and velocity. Nickel significantly improves the general corrosion resistance of stainless steels, by promoting passivation. Austenitic stainless steels therefore possess superior corrosion resistance when compared with martensitic or ferritic stainless steels.²⁹

2.3.2 Pitting Corrosion

Pitting corrosion is the result of the local destruction of the passive film and subsequent corrosion of the steel below. It generally occurs in chloride, halide or bromide solutions. Under certain conditions, particularly involving high concentrations of chlorides,

moderately high temperatures and low pH, localized corrosion can occur leading to perforation of the passive layer which might lead to severe corrosion that penetrates right through the cross section of the component. Grades high in chromium, and particularly molybdenum and nitrogen, are more resistant to pitting corrosion.

The mechanism of pitting attack of stainless steel has been divided into three consecutive steps: initiation, metastable propagation and stable propagation of pits. The initiation step is mainly a local breakdown of the passivation oxide layer in presence of aggressive anions (chloride anion) of the environment.³⁰ The corrosion rate is increased by the fact that even more aggressive environment is produced by the corrosion reaction itself. However, at the earlier stages of pit propagation, when the pits are still very small, they can be repassivated spontaneously. This stage is often referred as metastable pit growth. The stage of stable propagation is reached when spontaneous re-passivation is no longer possible.³¹

2.3.3 Crevice Corrosion

Similar to the pitting corrosion, this type of corrosion also initiates when the protective layer on the metal surface is destructed. The area or location where the oxide layer is destructed if associated with incomplete weld penetration or overlapping surfaces can form crevices which can promote corrosion. To function as a corrosion site, a crevice has to be of sufficient width to permit entry of the corroding media, but sufficiently narrow to ensure that the corroding media remains stagnant.³² Accordingly crevice corrosion usually occurs in gaps a few micrometers wide, and is not found in grooves or slots in

which circulation of the corrodent is possible. Crevice corrosion is a very similar mechanism to pitting corrosion; alloys resistant to one are generally resistant to both. Crevice corrosion can be viewed as a more severe form of pitting corrosion as it will occur at significantly lower temperatures than pitting.³³

Crevice corrosion has been one of the most serious problems when using stainless steels in chloride containing environments such as seawater. To avoid crevice corrosion, counter measures such as structural modification, improving the environment and material selection is used. On selecting materials with sufficient resistance to crevice corrosion in a given environment, it has been recognized that an increase in the content of alloying elements such as Cr, Mo and N improves crevice corrosion resistance.

Crevice corrosion tests on a range of commercial stainless steels in natural seawater found that the high Cr and Mo ferritic stainless steel have superior crevice corrosion resistance compared with the austenitic steels having similar Cr and Mo content.³⁴

2.3.4 Galvanic Corrosion

Corrosion in general is an electrochemical process involving the flow of electric current, corrosion can be generated by a galvanic effect which arises from the contact of dissimilar metals in an electrolyte (an electrolyte is an electrically conductive liquid).

Galvanic corrosion occurs when two dissimilar metals, or alloys are put in a common electrolyte, causing electric current to flow between them. When the current flows, material will be removed from one of the metals or alloys (Anode) and dissolve into the

electrolyte. The other metal (Cathode) will be protected. Metals and alloys are categorized to their susceptibility to galvanic corrosion in galvanic series.³⁵

Three conditions are required for galvanic corrosion to proceed; the two metals must be widely separated on the galvanic series, they must be in electrical contact and their surfaces must be bridged by an electrically conducting fluid. Removal of any of these three conditions will prevent galvanic corrosion.³⁶ Galvanic corrosion is also the method for cathodic protection by sacrificial anode.

Steel is frequently welded to construct a larger structure. During the construction process, welded materials are sometimes exposed to water in the environment. For example, steel frames of a building or bridge are sometimes exposed to rain water, river water, underground water and even seawater during the construction process before application of corrosion protection. The corrosion rate of a structure in such conditions depends on the composition, temperature and oxygen content of the water, and these parameters differ depending on location and season. When a welded structure is exposed to water containing corrosion-aggressive ions such as chloride ions, corrosion becomes severe even in a short period of exposure. In such a condition, localized corrosion such as galvanic corrosion coupled with reduction reaction of dissolved oxygen can occur because the welded structure is composed of different metals or has heterogeneity in the heat-affected zone induced by the welding process.³⁷

2.3.5 Intergranular Corrosion

This type of corrosion occurs in stainless steels as they all contain small amounts of carbon. It is a relatively rapid and localized corrosion associated with a defective microstructure known as carbide precipitation. When austenitic steels have been exposed to high temperatures for a period of time in the range of approximately 425 to 850°C, or when the steel has been heated to higher temperatures and allowed to cool through that temperature range at a relatively slow rate (welding or air cooling after annealing), the chromium and carbon in the steel combine to form chromium carbide particles along the grain boundaries throughout the steel. Formation of these carbide particles in the grain boundaries depletes the surrounding metal of chromium and reduces its corrosion resistance, allowing the steel to corrode preferentially along the grain boundaries. Steel in this condition is called sensitized.³⁸

Carbide precipitation depends upon carbon content, temperature and exposure time at these temperatures. The most critical temperature range is around 700°C, at which 0.06% carbon steels will precipitate carbides in about 2 minutes, whereas 0.02% carbon steels are effectively immune from this problem.³⁹

Intergranular corrosion in austenitic stainless steels is due to chromium depletion at the grain boundaries caused by chromium carbide precipitation. , when austenitic stainless steels are exposed for long periods in the range from 500 °C to 900 °C, the precipitation of a large number of phases, besides chromium carbide, might occur, such as inter-metallic phases. The susceptibility to intergranular corrosion is decreased in stainless steels by reducing their carbon content to less than 0.03 weight%; the main types of this stainless steel class are AISI 304L and 316L. Nevertheless, the decrease in carbon

content reduces still further the low yield strength of the austenite in these steels in the annealed condition. Nitrogen might be added in order to counteract this effect, as is the case with 316L (N). Nitrogen in solid solution in the austenite phase increases the strength, stabilizes the austenite and increases the pitting resistance.⁴⁰

2.3.6 Stress Corrosion Cracking

Stress corrosion cracking (SCC) is the degradation of the material under the combined action of a load and a corrosive medium, neither of which when acting alone would have caused the failure. It has a few typical characteristics. (i) it occurs only in specific media, corrosion rate and re-passivation rate, (ii) it occurs only in materials that show active-passive behavior, (iii) it is a macroscopically brittle failure that occurs in ductile materials, and (iv) it can occur at stress levels much below yield stress.^{41 42}

Corrosion has always been a problem in the petroleum refining and the petrochemical operations. The petrochemical process elements are frequently performed at high temperatures and in severely corrosive environments; therefore, heat- and corrosion-resistant alloys, e.g., austenitic stainless steels, have been used widely in the petrochemical industries because of their excellent mechanical strength and toughness⁴³. However, in chloride-containing high temperature environments, pitting, crevice corrosion^{44 45}, and stress corrosion cracking (SCC)⁴⁶ is often associated with the operation.

In addition, it was found that the factors most affecting corrosion of structural materials in the petrochemical industry is chloride (Cl^-) and hydrogen sulfide (H_2S). H_2S is an important constituent of refinery sour waters and is also formed by the decomposition of organic sulfur compounds that are present at elevated temperatures.

The most damaging environment is a solution of chlorides in water, particularly at elevated temperatures. As a consequence stainless steels are limited in their application for holding hot waters (above about 50°C) containing even trace amounts of chlorides (more than a few parts per million). This form of corrosion is only applicable to the austenitic group of steels and is related to the nickel content. Grade 316 is not significantly more resistant to SCC than is 304. The duplex stainless steels are much more resistant to SCC than are the austenitic grades, with grade 2205 being virtually immune at temperatures up to about 150°C , and the super duplex grades are more resistant again. The ferritic grades do not generally suffer from this type of corrosion.

Although limits has been established for use of certain types of stainless steel, an example, Grade 304 is being used in water containing 100 - 300 parts per million (ppm) chlorides at moderate temperatures; but it is very risky at conditions normally change in petrochemical processes, and the results might be catastrophic.

Recently there have been a small number of instances of chloride stress corrosion failures at lower temperatures than previously thought possible. These have occurred in the warm, moist atmosphere. Temperatures as low as 30 to 40°C have been involved. There have also been failures due to stress corrosion at higher temperatures with chloride levels as low as 10 ppm.

CHAPTER 3: Process Description

Condensate Recovery Plants are designed to separate light well fluids and recover them, the feed to such type of plants is normally from multiple gas wells which are distributed throughout the condensate rich gas reservoir. Recently the demand for condensate in the market has increased, as it became a feedstock to refineries to mix with heavy crude oil, or to chemical plants. Nowadays, with the rising prices of crude oil, condensate prices has also risen from 65\$ per barrel several years back, to over 120\$ per barrel today. Figure 11 is a block diagram of the condensate recovery plant from the battery limits.

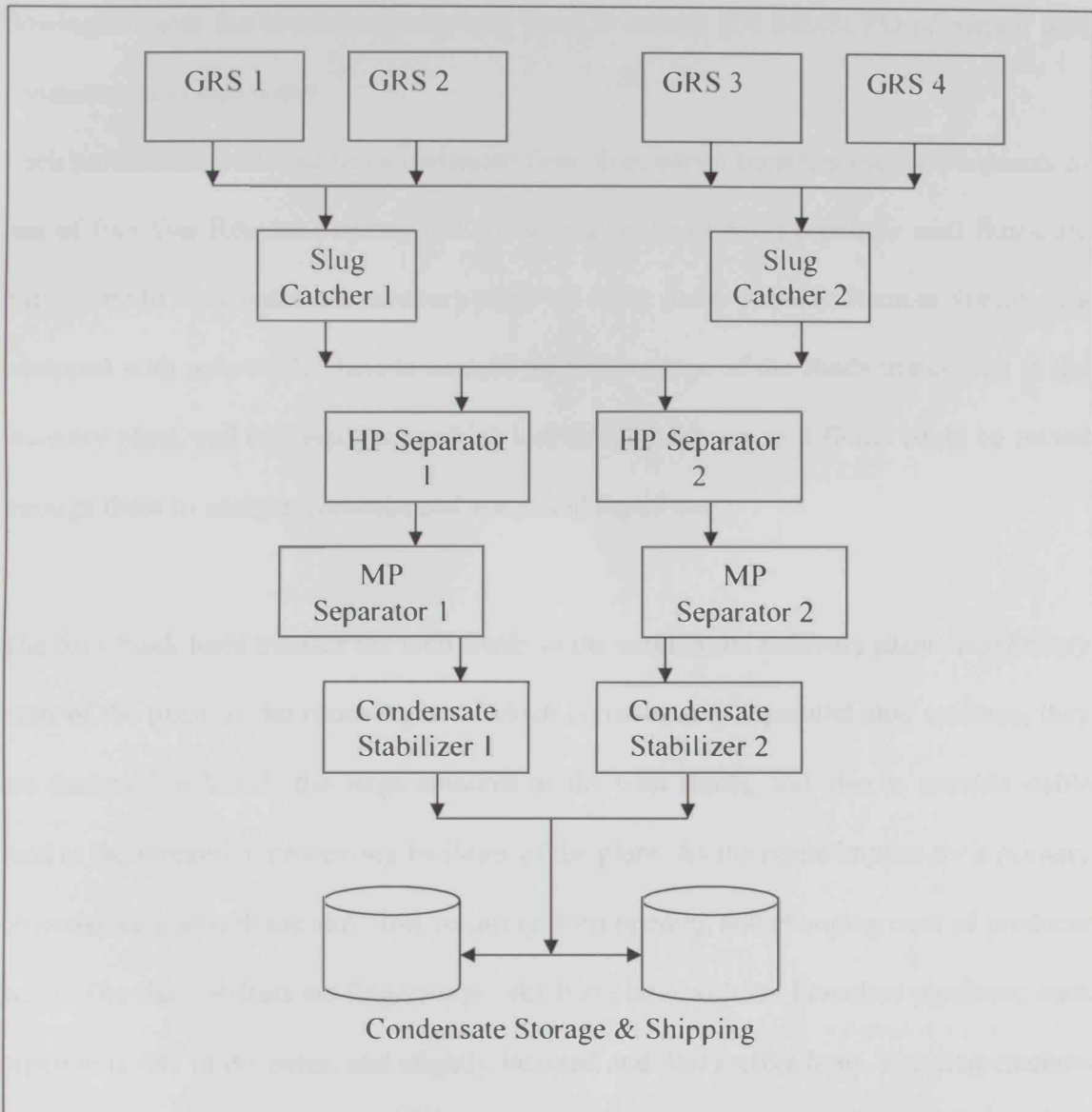


Figure 11: A block diagram of a condensate recovery plant.

3.1 Gathering System and Inlet Facility

The gathering system consists of a number of production wells, these wells are divided into gas producers from two different formations of the reservoir. The total production

flowing towards the condensate recovery plant is around 800 MMSCFD of natural gas, condensate and free water.

Each production wellhead has a dedicated flow line, which transfers the well contents to one of four Gas Remote Stations (GRS); several wells (4 to 9) producer well fluids are transferred to the condensate recovery plant via trunk lines. The Gas Remote Stations are equipped with only cooler fans to control the temperature of the fluids transferred to the recovery plant, and test separators which individual producer well fluids could be routed through them to analyze contents, and water and liquid cuts.

The four trunk lines transfer the well fluids to the condensate recovery plant. The battery limit of the plant, is the receiving area which consists of two parallel slug catchers, they are designed to handle the large amounts of the well fluids, and also to provide stable feed to the remaining processing facilities of the plant. As the name implies their primary objective is to absorb the slug flow resulting from opening and changing over of producer wells. The slug catchers are fingers type which are large volume branched pipelines; each pipeline is 48" in diameter, and slightly inclined and 300 meters long. The slug catchers have capacity to handle more than 70,000 barrels of liquid each.



Figure 12: Slug Catcher at the condensate recovery plant battery limit

3.2 High Pressure Separation

The liquids (condensate and water) from the slug catchers along with the gas are routed to two High Pressure (HP) separators. The separators are three phase separators, and a preliminary separation is achieved in them. The HP separators are equipped with a water boot to collect water, a mist eliminator to prevent liquid particles to go with the gas, and vortex breaker at the liquid outlet. The residence time in the HP separator is around 7 minutes, allowing the water to settle by gravity at the bottom, the condensate on top of water, and the gas on top.

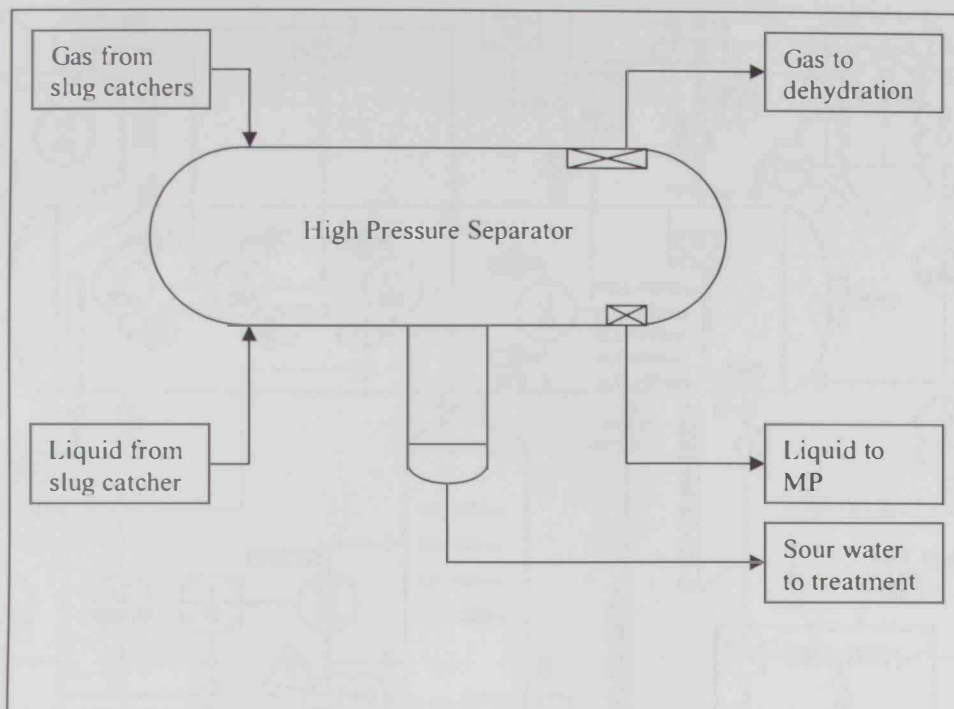


Figure 13: Process Flow Diagram of the high pressure separator

The pressure in the HP separator is around 70 bars, and the temperature is maintained at 50°C. The following table shows the design parameters of the high pressure separator.

Design Parameter	
Inner Diameter	3.8 meters
Length	15 meters
Boot Inner Diameter	1.2 meters
Boot Length	1.8 meters
Design Pressure	84 Bars
Design Temperature	195°C

Table 3: Design parameters of high pressure separator

Figure 13 is a section of the Piping and Instrumentation Diagram (PID), which show the different transmitters, and interlocks installed at the high pressure separator. Those instrumentation include level transmitters, level controllers, level glasses, pressure indicators, and emergency shutdown interlocks.

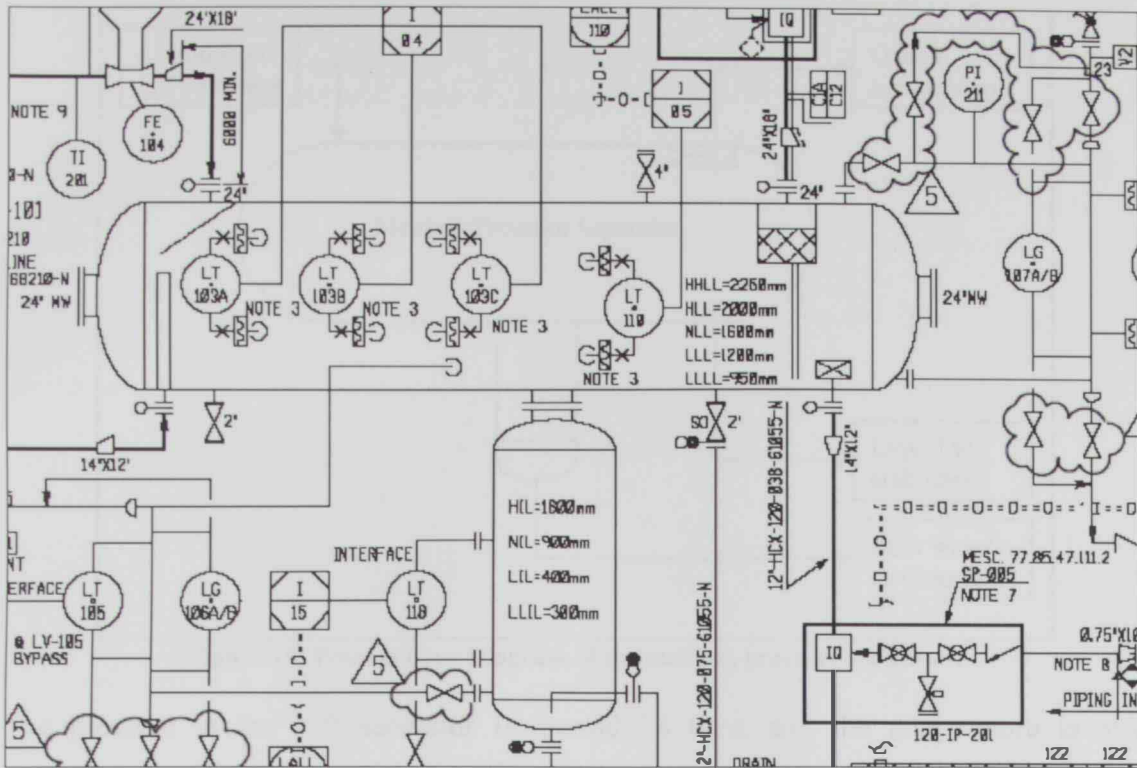


Figure 14: A section of Piping and Instrumentation Diagram (PID) of HP separator

3.3 Medium Pressure Separation

The liquids from the HP separators are routed to the Medium Pressure (MP) separator; it is similar in principle to the HP separator being a three phase separator. The reduction of pressure leads to a flashing effect, and more condensate condenses in the vessel. The medium pressure separator is also equipped with a water collection boot, a vortex breaker, and a mist eliminator.

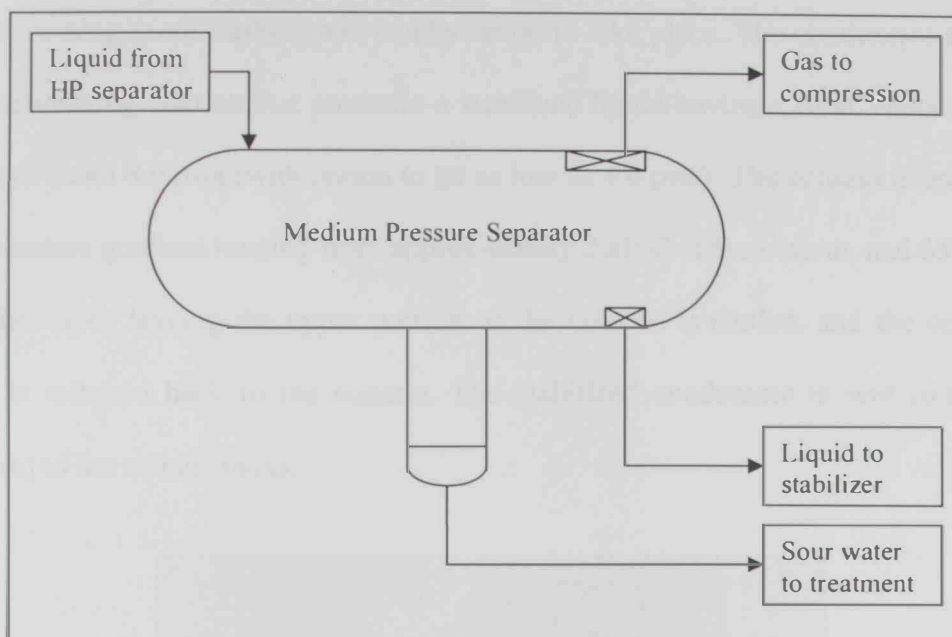


Figure 15: Process Flow Diagram of the medium pressure separator.

The pressure in the MP separator is around 28 bars, and the temperature is also maintained at 50°C. The MP separator is larger in volume than the HP separator, this is due to larger volumes of condensate and water that are condensed in this section of the process as the pressure is reduced. The following table shows the design parameters of the medium pressure separator.

Design Parameter	
Inner Diameter	3.9 meters
Length	19 meters
Boot Inner Diameter	1.2 meters
Boot Length	2.1 meters
Design Pressure	32 Bars
Design Temperature	195°C

Table 4: Design parameters of medium pressure separator

3.4 Condensate Stabilization

The liquids from the MP separator (which is mainly un-stabilized condensate with traces of water) are routed to the condensate stabilizer, where the pressure is further reduced to

11 bars causing more flashing and condensation to take place. The condensate stabilizer is a fractionating column that produces a stabilized liquid having a Reid Vapor Pressure (RVP) of about 8.0 psia (with option to go as low as 4.0 psia). The column is operated at a temperature gradient ranging from approximately 200° C at the bottom, and 65°C at the top. The vapor leaving the upper portion of the column is cooled, and the condensed liquid is refluxed back to the column. The stabilized condensate is sent (differential pressure) to the storage tanks.



Figure 16: Condensate Stabilizer

The main features of the stabilizer section include:

Two re-boilers at the bottom, overhead condenser and reflux drum at the top, two water draw off drums, and two side heat exchangers (inlet outlet heat exchangers). The heat exchangers (side and bottom) along with the condenser maintain the temperature profile throughout the fractionation column, and the process is optimized by controlling the reflux rate, and the re-boiler duty to maintain temperature profile. The side heat exchangers work as pre-heaters at one side of the stream, and pre-coolers at the other stream, they are designed to optimize the energy used for heating and cooling. The water draw off drums are designed to hold and capture the remaining water that was not separated in the previous separation areas (high and medium separation), the draw off drums are horizontal vessels equipped with level controllers to maintain the water level at a certain level, whereas the condensate is sent through the top.

The liquid export specification can be varied by changing the temperature and pressure operating conditions of the stabilizer column; normally it is only the temperature that is controlled while maintaining the pressure fixed. The following table includes the design parameters of the condensate stabilizer.

Design Parameters	
Height	45 meters
Inner Diameter	4.4 meters (bottom) : 1.8 meters (top)
Capacity	450 cubic meters of liquids
Design Pressure	15 Bars
Operating Pressure	12 Bars
Hydrostatic test pressure	27 Bars
Design temperatures	343°C (bottom); 260°C (top)
Operating temperatures	220°C (bottom); 650°C (top)
Corrosion allowance	1.6 mm

Table 5: Design parameters of condensate stabilizers

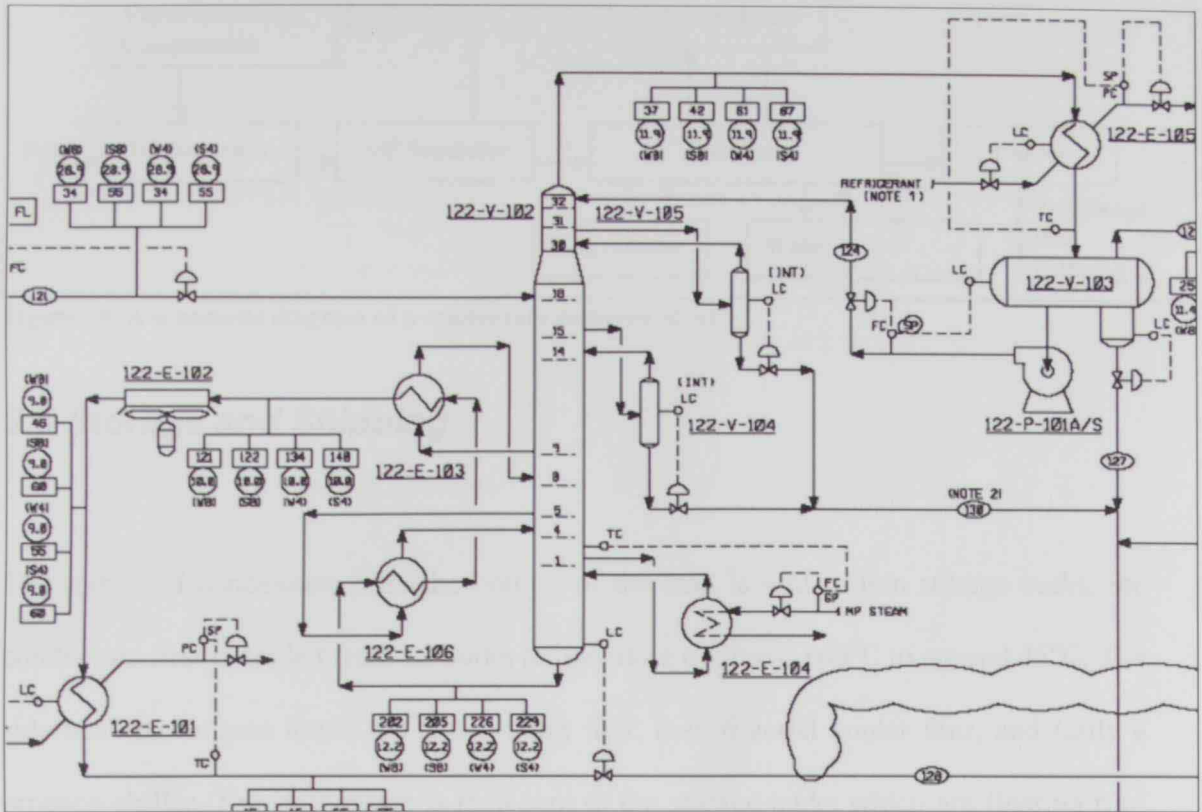


Figure 17: PFD of overall stabilization section



Figure 18: Condensate stabilizer columns under construction

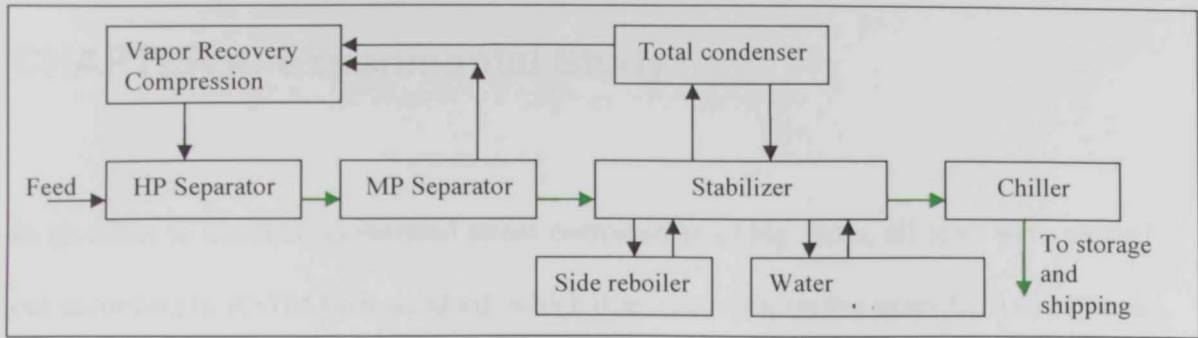


Figure 19: A schematic diagram of a condensate recovery plant

3.5 Storage and Shipping

The stabilized condensate from the bottom of the tank is sent to two storage tanks, the condensate first is cooled from its outlet temperature of above 160°C to around 45°C. The side heat exchangers lower the temperature first, then 6 aerial cooler fans, and lastly a propane chiller. The condensate is then sent to the storage tanks which are floating roof type tanks. The storage tanks provide the necessary head pressure for the booster pumps and main pumps to transfer the condensate to downstream refinery.

CHAPTER 4: Experimental Study

In an effort to conduct accelerated stress corrosion cracking tests, all tests were carried out according to ASTM G36 standard, which does not replicate the exact field conditions, but provides us with guidelines in which the material possesses better stress corrosion resistivity.

Stress corrosion cracking was evaluated for stainless steel 316L and Inconel (Nickel alloy) in boiling magnesium chloride solution according to ASTM G36 standard⁴⁷. This method was used as this environment provides an accelerated method of ranking the relative degree of stress corrosion cracking susceptibility for stainless steels and related alloys in aqueous chloride containing environments. This method was also used as the test is applicable to wrought, cast, and welded stainless steel and related alloys. It is a method for detecting the effects of composition, heat treatment, surface finish, microstructure, and stress on the susceptibility of these materials to chloride stress corrosion cracking.

The following paragraphs show in details the materials used, and elaborate on the method of testing.

4.1 Materials

Stainless steel 316L and Inconel 625 were used in the boiling magnesium chloride immersion tests. The materials were purchased in sheet shapes from McMaster Company, USA.

The sheets were fabricated into U-Bends at Jaguar Industrial Workshop in Sharjah, UAE.

The specifications of the purchased materials are shown in table 6.

Material	Super Corrosion-Resistant Stainless Steel (Type 316L)	High-Strength, Ultra Corrosion- Resistant Nickel (Alloy 625) INCONEL
Shape	Sheet	Sheet
Thickness	0.12"	0.2"
Length	1'	1'
Hardness	217 Brinell	220 Brinell
Yield Strength	25,000 psi	55,000 psi
Condition	Cold Finished Condition (Annealed)	Cold Finished Condition (Annealed)
Specification	ASTM A240	ASTM B443

Table 6: Material specification of stainless steel 316L and inconel 625

4.1.1 U-Bends

U-Bend specimens were prepared from the sheets mentioned in the previous part to conduct the stress corrosion tests. The preparation of the U-bend specimens was done according to the procedures mentioned in the ASTM G30-97.⁴⁸ The U-Bend specimen is generally a rectangular strip which is bent 180° around a predetermined radius and maintained in this constant strain condition during the stress-corrosion test.

The selection of U-Bends for the stress corrosion tests was mainly because the U-bend specimens usually contain both elastic and plastic strain; whereas other stress corrosion specimens such as the direct tension specimens, or the bent-beam specimens are normally used to study stress-corrosion cracking of strip or sheet under elastic strain only. The following figures show the method used for tensioning and bolting of U-Bend samples.

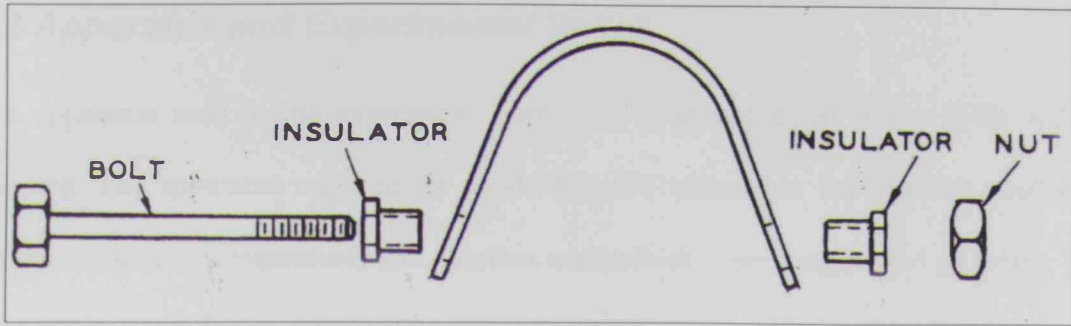


Figure 20: Method of bolting and stressing the U-Bends

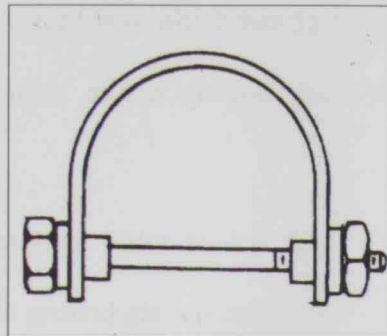


Figure 21: Final U-Bend shape after stress is applied

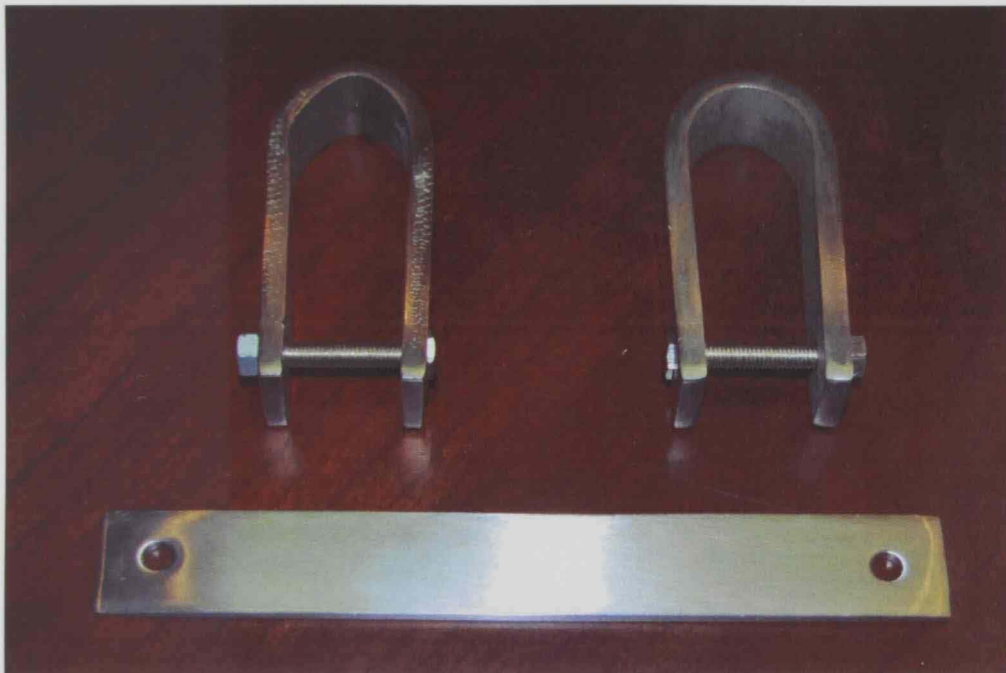


Figure 22: U-Bend specimens of stainless steel 316L, and inconel 625

4.2 Apparatus and Experimental Setup

The apparatus used in the experiment were exactly as suggested in the G-36 ASTM standard. The apparatus required for conducting the immersion experiments needed to maintain constant temperature, and solution concentration for long period of times. The following are the design details of the apparatus used:

- Flask: a 1 Liter Erlenmeyer Flask which has a ground glass 45/50 outer joint at the mouth for the condenser, and a ground glass 10/30 outer joint to hold the thermometer.
- Condenser: a 250 mm long water cooled condenser with a 45/50 ground glass inner joint, and a 29/26 ground glass outer joint to hold the trap.
- Trap: a trap to contain at least 25 weight percent of the solution to be placed on top of the condenser to eliminate vapor losses. The trap is joined to the condenser by a 29/26 ground glass inner joint.
- Thermometer: a graduated thermometer to monitor and adjust the boiling temperature of the solution.

The following are some pictures of the assembled apparatus:

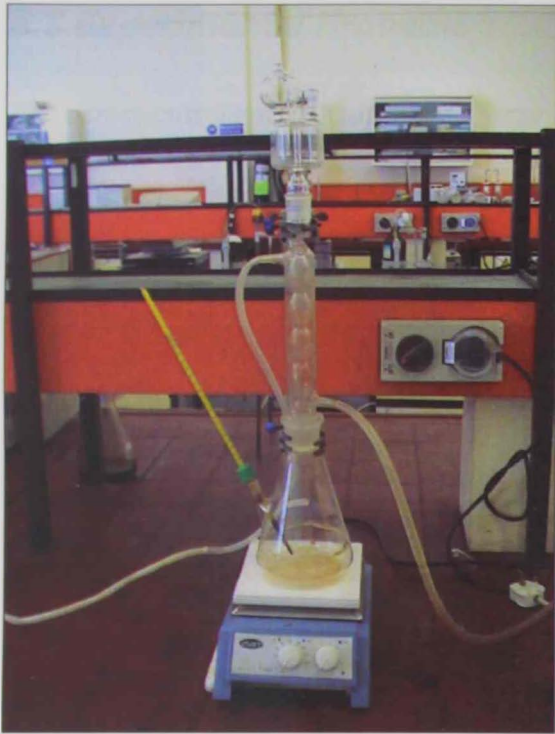


Figure 23: Assembled apparatus as per ASTM G-36

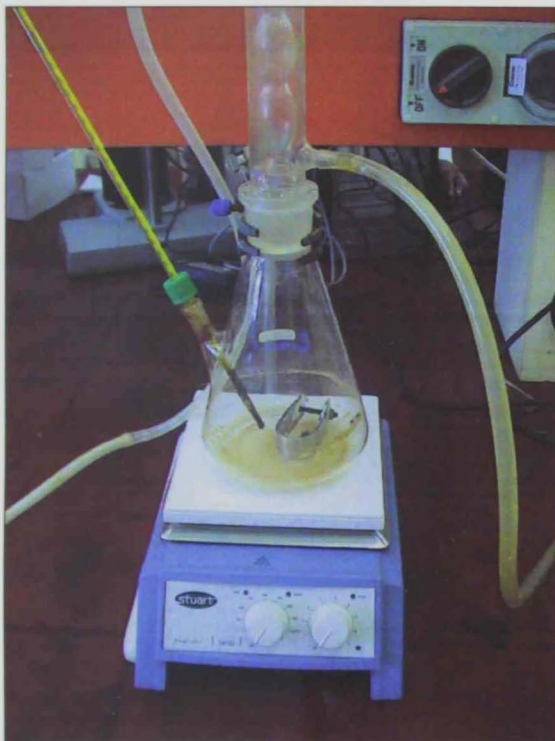


Figure 24: Assembled apparatus with a close up of water condenser and trap

4.3 Experimental Procedure

The stress-corrosion cracking tests were carried out in a boiling magnesium chloride solution; the test solution was held at a constant boiling temperature of 155.0 ± 1 °C. The solution was prepared by adding a predetermined quantity of reagent grade magnesium chloride ($\text{MgCl}_2 \cdot 6\text{H}_2\text{O}$) to distilled water into the flask (mentioned in apparatus). The apparatus was placed on a heat source as shown in figure 24. When magnesium chloride solution started boiling, it was adjusted to maintain the boiling point at 155.0°C through the addition of small quantities of distilled water.

The stressed U-bend specimens were added after the solution was stabilized at the desired boiling point. The test solution was changed weekly in order to maintain the same concentration throughout the test period.

One specimen per flask was used, and the specimens were removed once daily to inspect and check for cracks⁴⁹. The crack initiation time for each specimen was recorded, along with the type of specimen, and time of exposure. The samples were removed as soon as the crack initiated; the samples were then cut into sections in order to fit the SEM chamber. The tests were carried out at the end of the experimental procedure to inspect crack initiation.

CHAPTER 5: Results and Discussion

5.1 Feed Analysis

Titrimetric method of AgNO_3 and Potassium chromate indicator was used to calculate the chloride concentration in the water samples taken from the water draw off drums of the stabilizer columns. Several samples were taken from each train, the following are the results:

	Train1: Draw off drum (PPM)	Train2: Draw off drum (PPM)
1	13	35
2	17	14
3	20	17
4	18	18

Table 7: Chloride content in water samples from draw off drums of both stabilizers

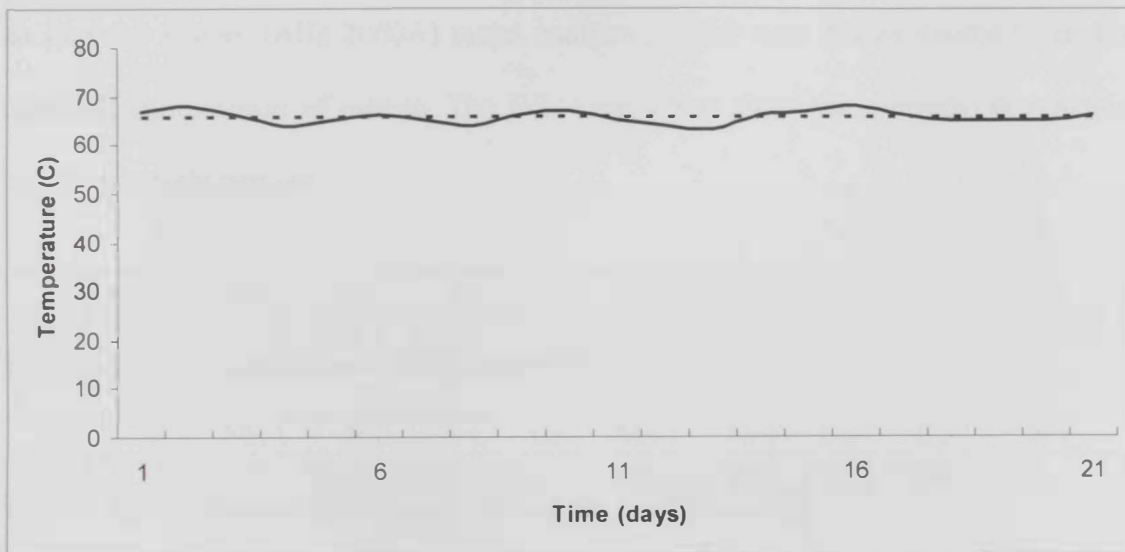


Figure 25: A three week temperature trend of the top part of the condensate stabilizer

The water samples all resulted with low concentrations of chlorides, although the design criteria considers higher chloride contents and H_2S concentrations, yet stainless steel (316L) underwent stress corrosion cracking. The austenitic stainless steels are susceptible

to stress corrosion cracking, and the conditions in the top part of the stabilizer aggravate the corrosion like the presence of chlorides along with high temperatures above 65°C (figure 25 shows a three week trend for the temperature of the top side of the stabilizer column with an average of 66°C), hydrogen sulfide and tensile stress. The tensile stresses are resulted from the residual stresses due to fabrication cold working processes and applied bolting tension stresses; this could be concluded from all the cracks that took place in the cold bent section and around the bolt circle in all the clips.

5.2 Chemical Composition

The chemical composition of materials used in all the experiments were analyzed using an Innovax system (Alfa 2000A) metal analyzer; which uses X-Ray source to analyze chemical composition of metals. The following tables show the chemical composition results in weight percent.

C	SI	Mn	P	S	Cr	Mo	Ni	Cu	Co	N	Fe
0.03	0.75	1.21	0.04	0.03	15.7	2.02	10.23	0.31	0.08	0.1	71.77

Table 8: Chemical composition of original stainless steel 316L clip

C	SI	Mn	P	S	Cr	Mo	Ni	Cu	Co	N	Fe
0.03	0.75	1.22	0.04	0.03	16.11	2.05	9.69	0.31	0.08	0.1	71.56

Table 9: Chemical composition of purchased stainless steel 316L sample

Comparing the first two tables, which were of the original stainless steel 316L clip and the sample material purchased, show that the material contained similar compositions of alloying elements, which confirms that the material used in the stabilizer column clips

and the material used for U-bend testing were similar in concentration of alloying elements, and they both were made of stainless steel 316L.

C	SI	Mn	P	Ti	Cr	Mo	Ni	Cu	Co	Nb	Fe
0.1	0.5	0.5	0.15	0.21	28.82	9.86	58.77	0.00	1.00	3.43	3.48

Table 10: Chemical composition of inconel 625 sample

The inconel; which is a nickel alloy, has a high concentration of nickel as an alloying element. Moreover, it has high percentage of chromium and minute percentages of titanium and iron.

5.3 Stress Calculation

The U-Bends were stressed to shape shown in figure 26 using the method mentioned in the ASTM G 30-97 standard. All specimens were held to their configuration using bolts and nuts made of stainless steel 316L, which were tightly screwed within plastic gaskets. The strain ϵ , on the outside of the U-Bend was calculated using the following equation.⁴⁵

$$\epsilon = \frac{T}{2R} \quad \text{Equation 1}$$

Where T is the specimen thickness and R is the inner radius of the U-Bend curvature in mm.

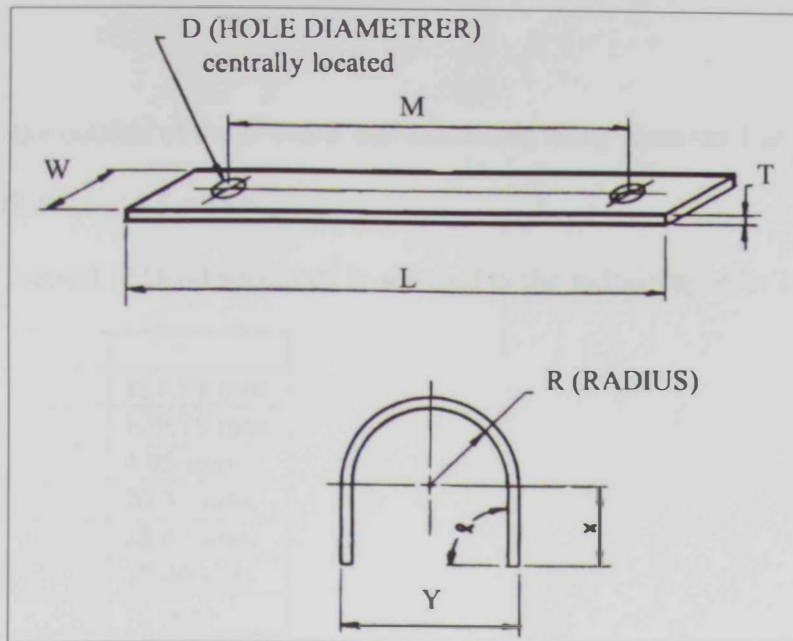


Figure 26: Geometry of a U-Bend specimen

As the materials were not available in the market in the same thickness, the amount of stress on each specimen was kept constant at the same strain rate; this was achieved by reducing the U-Bend radius of the stainless steel specimen. The following tables show the average geometries of the specimens.

Stainless Steel 316L

The strain on the outside of the U-Bend was calculated using equation 1 as follows:

$$\epsilon = T/2R = 3.17/2 \times 10 = 15.8 \approx 16\%$$

Geometry of U-Bend specimen is attached in the following table:

L	152.01 mm
M	130.94 mm
T	3.17 mm
W	19.80 mm
X	51.03 mm
Y	37.75 mm
R	10 mm

Table 11: Dimensions of U-Bend specimens (average of 6 specimen)

Inconel 625

The strain on the outside of the U-Bend was calculated using equation 1 as follows:

$$\epsilon = T/2R = 4.95/2 \times 15 = 16.5 \approx 16\%$$

Geometry of Inconel U-Bend specimen is attached in the following table:

L	151.51 mm
M	129.75 mm
T	4.95 mm
W	20.32 mm
X	48.63 mm
Y	42.40 mm
R	15 mm

Table 12: Dimension of inconel U-Bend specimens (average of 6 specimens)

5.4 Crack Initiation Tests

As detailed in the experimental part, the stress-corrosion cracking tests were carried out in a boiling magnesium chloride solution; the test solution was adjusted to maintain the boiling point at 155.0°C. The stressed U-bend specimens were added after the solution stabilized at the desired boiling point. The test solutions were changed weekly in order to maintain the same concentration throughout the test period. Each specimen was tested in separate flask, and the specimens were removed once daily to inspect and check for cracks. The crack initiation time for each specimen, along with the type of specimen and times of exposure were recorded, the following table shows the results:

Stainless Steel 316 L		Inconel (625 alloy)	
Specimen	Time to initiate crack	Specimen	Time to initiate crack
1	21 days	1	58 days
2	24 days	2	53 days
3	23 days	3	64 days
4	27 days	4	59 days
5	23 days	5	49 days
6	24 days	6	54 days
average	24 days	average	56 days

Table 13: Crack initiation time for specimen in boiling magnesium chloride solution

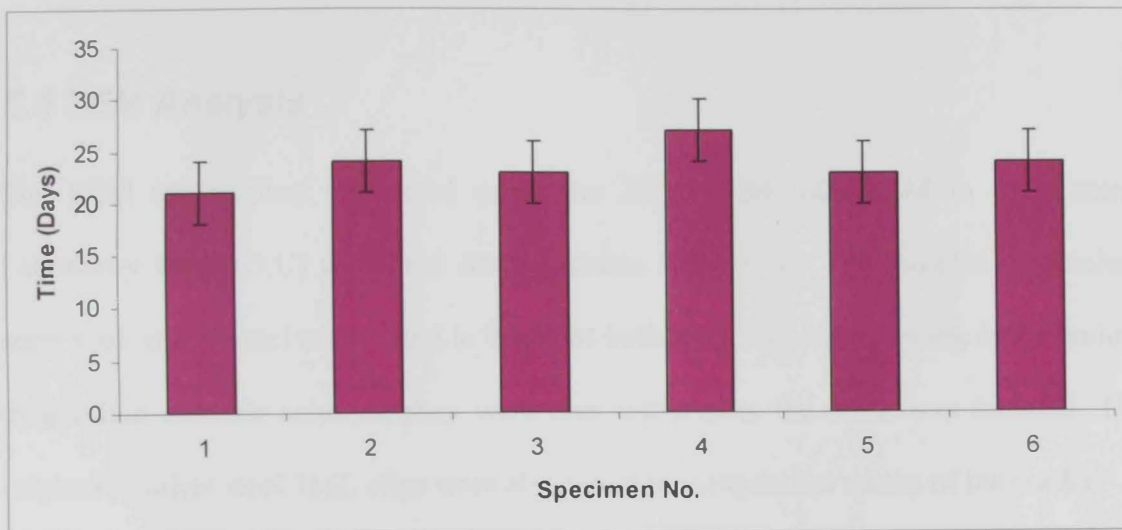


Figure 27: Crack initiation time for stainless steel 316L U-Bend specimen in solution

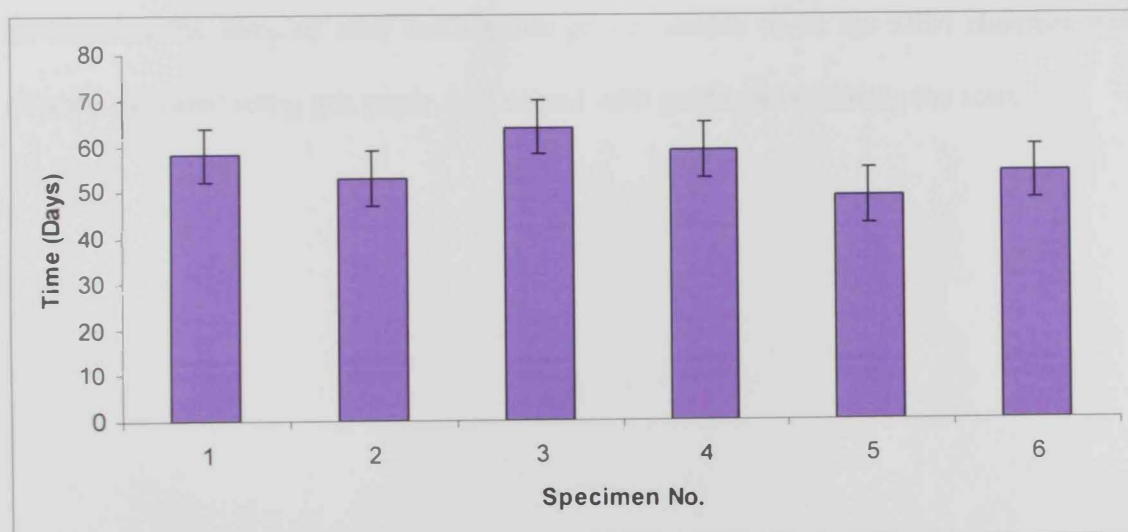


Figure 28: Crack initiation time for inconel U-Bend specimen in solution

The average crack initiation times for the stainless steel 316L and inconel U-bend samples were 24 and 56 days, respectively. The inconel samples showed better corrosion resistance in the boiling magnesium chloride solution. As this test provides an accelerated environment for stress corrosion, it can be concluded that inconel is more suitable for chloride containing environments than stainless steel 316L, where stress corrosion cracking is predictable.

5.5 SEM Analysis

The SEM testing was conducted using the JEOL JSM-5600 SEM in the Central Laboratory Unit (CLU) at United Arab Emirates University. The samples of stainless steel 316L and inconel were tested in the SEM before the immersion testing in the boiling magnesium chloride solution; they were also tested after the crack was initiated. The original stainless steel 316L clips were also tested to compare the nature of the cracks.

All specimens were prepared for the SEM testing according to ASTM G 1-03 standard; furthermore the samples after cutting into proper shapes to fit the SEM chamber were cleaned, polished using grit paper, and coated with gold before starting the tests.

Surface

The following pictures are SEM Macrographs of the surface of the U-bend samples before conducting the boiling magnesium chloride test.

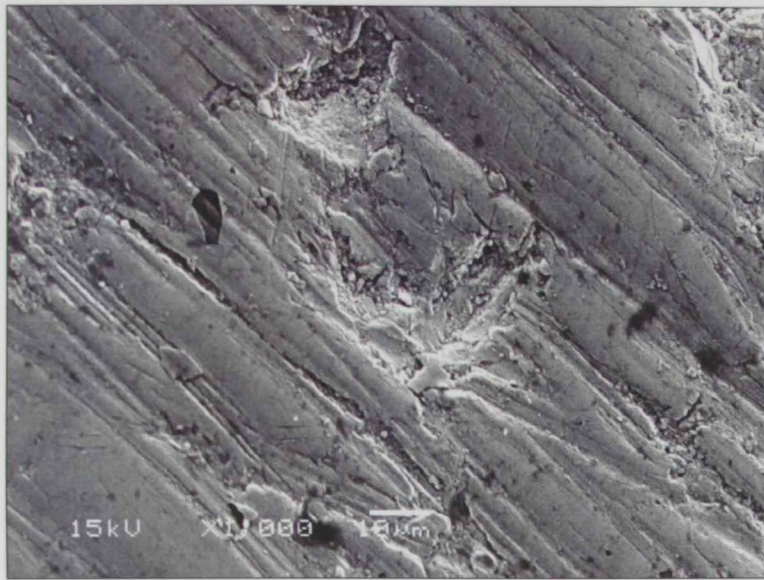


Figure 29: Macrograph of the surface of stainless steel 316L. (Resolution 1000)

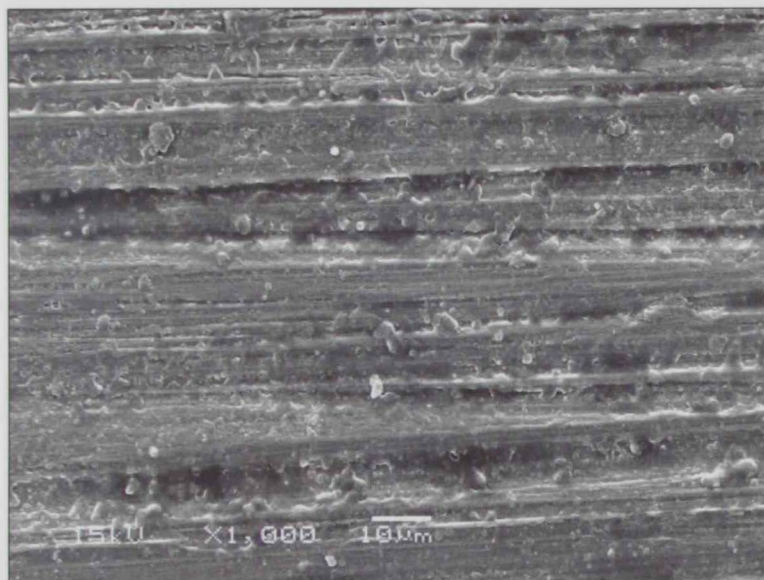


Figure 30: Macrograph of the surface of Inconel 625 (Resolution 1000)

Cracks of Controlled Samples

The following pictures are SEM Macrographs at different resolutions of the cracks occurred to the U-bend specimen in the boiling magnesium chloride solution.

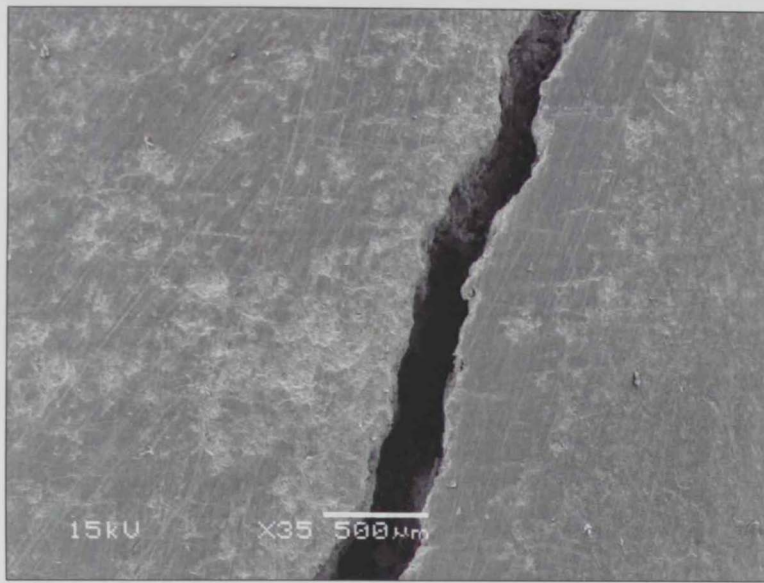


Figure 31: Macrograph of the crack of controlled stainless steel 316L. (Resolution 35)

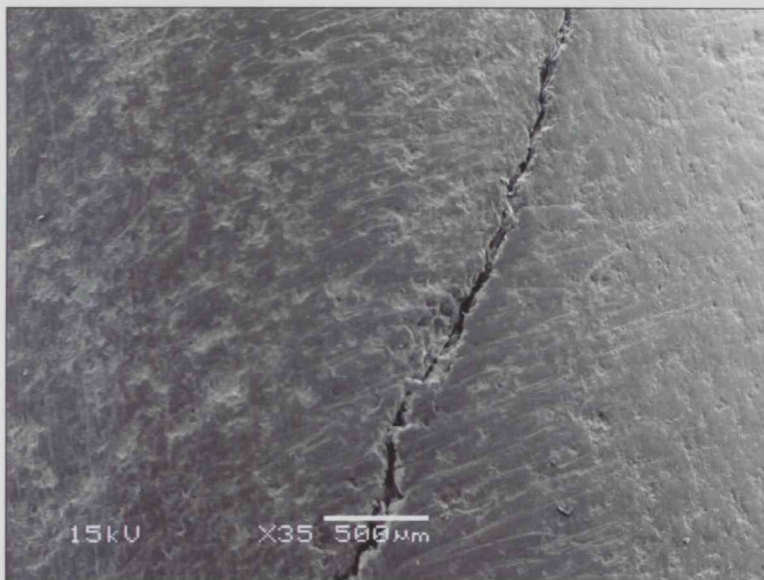


Figure 32: Macrograph of the crack of controlled Inconel 625 (Resolution 35)

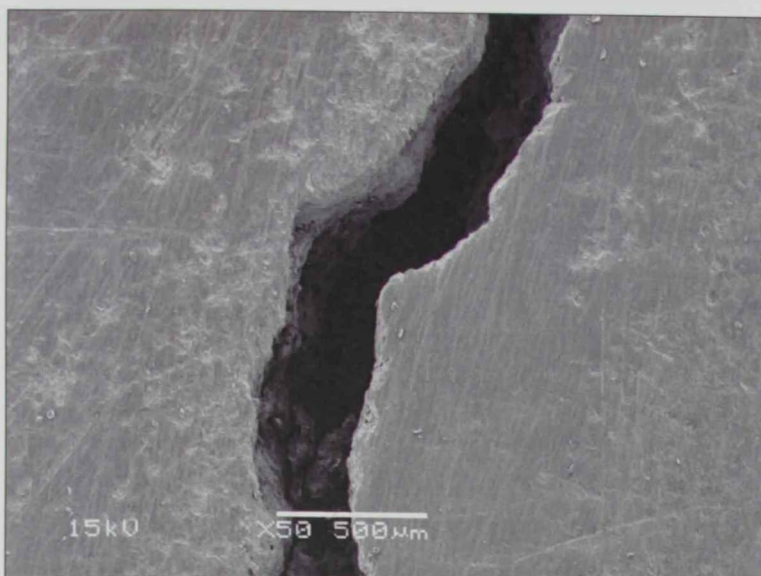


Figure 33: Macrograph of the crack of controlled stainless steel 316L. (Resolution 50)

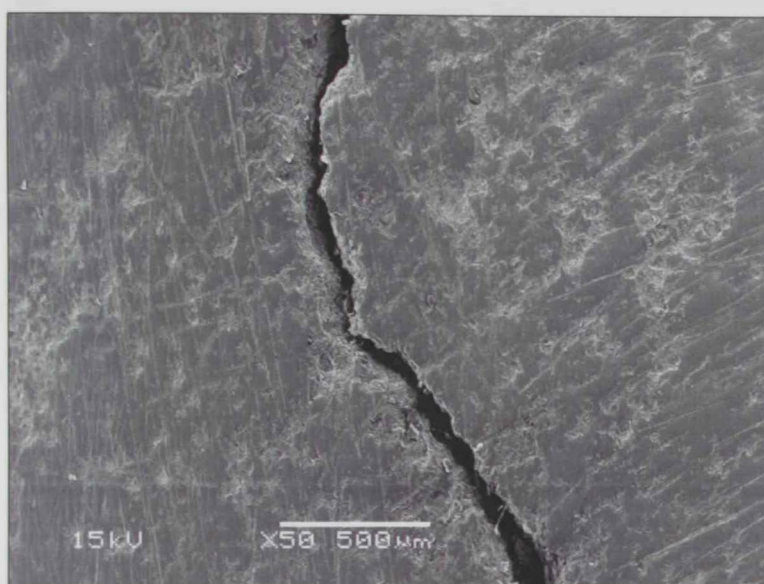


Figure 34: Macrograph of the crack of controlled inconel 625 (Resolution 50)

The stainless steel 316L samples were tested after an average of 24 days immersion test in the boiling magnesium chloride solution, compared to an average 56 days for the inconel samples. From the previous macrographs it is obvious that the cracks in stainless steel 316L samples are deeper, wider, and longer compared to inconel.

Cracks of Original Samples

The following pictures are SEM Macrographs at different resolutions of branched cracks of original stainless steel 316L clips at different resolutions.

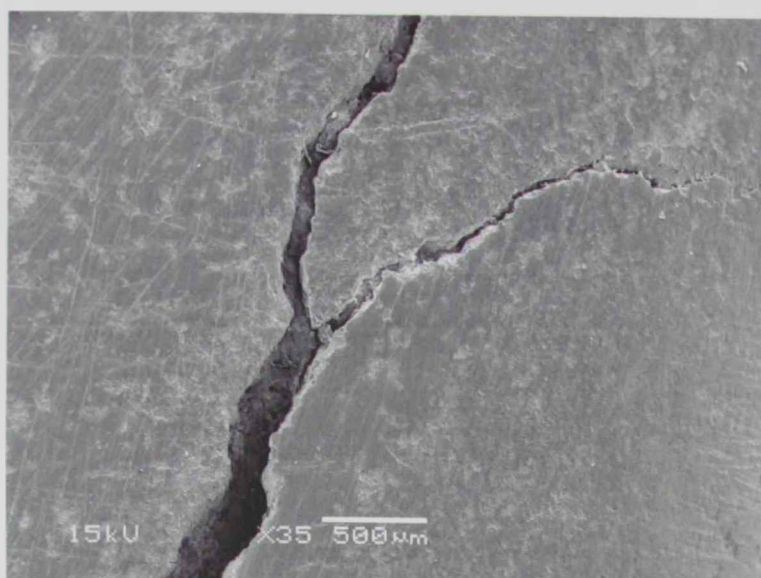


Figure 35: Macrograph of original crack of stainless steel 316L clip (Resolution 35)

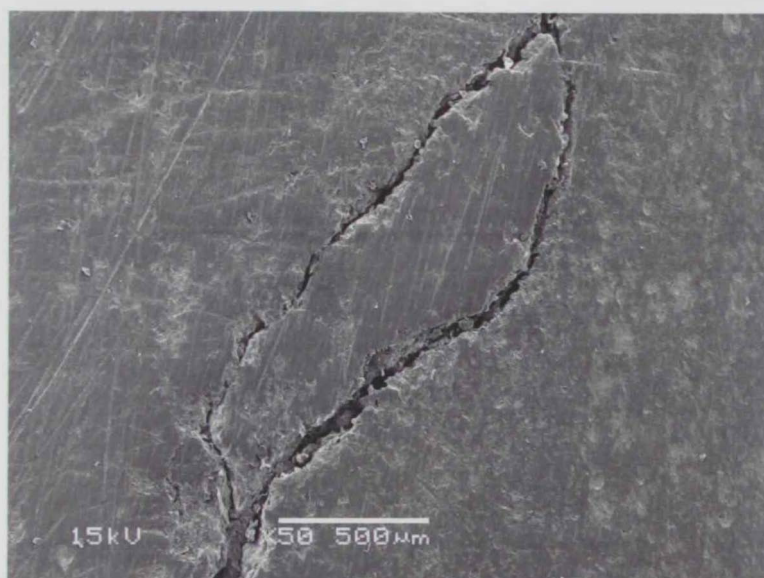


Figure 36: Macrograph of original crack of stainless steel 316L clip (Resolution 50)

The original failed stainless steel 316L clips obtained from the condensate stabilizer were also tested by the SEM. The samples were cleaned, polished, and cut to fit in the chamber

of the SEM. The macrographs above show similar nature of cracks resulted in testing the controlled sample of stainless steel 316L in the boiling magnesium chloride solution. However, the original clip cracks were longer in length and of a branched type.

CHAPTER 6: Conclusions and Recommendations

- From the results obtained from experiments conducted on the sample materials and feed analysis it was obvious that the main mode of failure was stress corrosion cracking initiated by the presence of chlorides, hydrogen sulfide, and water at elevated temperatures.
- Stress corrosion cracking was simulated in boiling magnesium chloride solution according to ASTM G36 standard which provides an accelerated corrosion environment. Although it does not replicate the exact same feed conditions where the material failure occurred, yet it provides guidelines to which materials have greater resistivity to this type of corrosion. Two candidate materials; stainless steel 316L (the original material) and inconel, were tested and evaluated. Based on the results obtained from the boiling magnesium chloride testing, inconel showed better corrosion resistance; an average of 56 days of immersion testing was required for the crack to initiate; compared to 24 days for a crack to initiate in the stainless steel 316L.
- The main reason for the above conclusion is the higher concentrations of Nickel and Chromium in inconel.
- The SEM micrographs showed that the cracks in stainless steel 316L samples were deeper, wider, and longer than those in the inconel samples. Furthermore, it

was noticed that the cracks in the stainless steel 316L samples showed branching, which in some cases may lead to spalling.

Since this study does not replicate the exact conditions of the stabilizers, it is recommended to implant inconel samples in the stabilizer during the unit shutdown and compare them after one year of service with the original 316 stainless steel samples.

Furthermore, it is recommended to study the crack propagation rate for both materials under the same conditions according to the ASTM G-36 standard.

It is also recommended to upgrade the stabilizer upper section internals to a higher corrosion resistant material, such as inconel; in order to minimize the production losses caused by the repetitive failure of the vessel internals. Moreover, installing chloride content analyzer at suspected areas or de-salters at upstream locations will be of a great importance; as it will indicate any process disturbance early.

References

¹ Energy Agency, Oil Market Report (Paris, France, May 2006), p. 14.

² Anthony H. Cordesman, Energy Developments in the Middle East, Greenwood Publishing Group, first edition, (2004)

³ "Worldwide Look at Reserves and Production," Oil & Gas Journal Vol. 104 No. 47 (2006) 24-25

⁴ Energy Information Administration, "International Petroleum (Oil) Reserves and Resources

⁵ Anthony Cordesman and Khalid Alrodhan, The Changing Dynamics of Energy in the Middle East, Praeger Security International, (2006)

⁶ John Calvert, The Arabian Peninsula in the Age of Oil (Library Binding), Mason Crest Publishers, (2007)

⁷ Historic Congressional Study: *Corrosion costs and Preventive Strategies in the United States*, a Supplement to Materials Performance, NACE International, Houston TX, July , (2002)

⁸ J. Beddoes and J. Gordon, Introduction to Stainless Steels, ASM International, Third edition (1999)

⁹ William.D.Callister, Material Science and Engineering an Introduction, fourth edition, willie, (1997)

¹⁰ H S Khatak and B Raj, Corrosion of austenitic stainless steel: Mechanism, mitigation and monitoring, Indira Gandhi Centre for Atomic Research, (2002)

¹¹ Serope Kalpakjian and Steven Schmid, Manufacturing Process for Engineering Materials, Prentice Hall, fourth edition, (2003)

¹² P. Marcus, I. Olefjord, "A Round Robin on combined electrochemical and AES/ESCA characterization of the passive films on Fe–Cr and Fe–Cr–Mo alloys", Corrosion Science 28 (1988) 589–602

¹³ P. Marshall, Austenitic Stainless Steels: Microstructure and mechanical properties, Springer, first edition, (1984)

¹⁴ D. Scott Mackenzie and George E. Totten, Analytical Characterization of Aluminum, Steel, and Superalloys, CRC; first edition, (2005)

¹⁵ M.P. Satish Kumar, P. Bala Srinivasan, "Corrosion behaviour of a thin section martensitic stainless steel GTA weldment in chloride solutions", *Materials Letters* 62 (2008) 2887–2890

¹⁶ A.K. Khare, *Ferritic Steels for High-Temperature Applications*, ASM International, (1983)

¹⁷ Norman Bailey, *Weldability of Ferritic Steels*, ASM International, (1994)

¹⁸ J.W. Martin *Precipitation Hardening: Theory and Applications*, Butterworth-Heinemann College; second edition, (1998)

¹⁹ M. Esfandiari, H. Dong , "The corrosion and corrosion–wear behaviour of plasma nitrided 17-4PH precipitation hardening stainless steel", *Surface & Coatings Technology* 202 (2007) 466–478.

²⁰ Robert Gunn, *Duplex Stainless Steels: Microstructure, Properties and Applications*, Woodhead Publications, (1998)

²¹ Deng et al., "Critical pitting and repassivation temperatures for duplex stainless steel in chloride solutions", *Electrochimica Acta* 53 (2008) 5220–5225

²² C.R. Brooks, Heat treatment, structure and properties of nonferrous alloys, ASM International, New York, (1984)

²³ R. Gibala and R. Hehemann, The Alloy Tree: A Guide to Low-Alloy Steels, Stainless Steels, and Nickel-base Alloys, CRC, first edition, (2004)

²⁴ Roger C. Reed, The Superalloys: Fundamentals and Applications Cambridge University Press, first edition, (2006)

²⁵ Al-Fadhli HY, Stokes J, Hashmi MSJ, Yilbas BS. "The erosion–corrosion behaviour of high velocity oxy-fuel (HVOF) thermally sprayed inconel-625 coatings on different metallic surfaces", Surface Coating Technology 200 (2006) 5782-5788

²⁶ Çam and M. Koçak, "Progress in joining of advanced materials", International Material Revision 43 (1998) 1–44

²⁷ H.L. Eiselstein and D.J. Tillack, Superalloy 718, 625 and various derivatives, TMS, Warrendale PA, (1991)

²⁸ A. John Sedrics, Corrosion of Stainless Steels, John Wiley and Sons, Inc. (1996)

²⁹ Catherine Houska, Stainless steels in architecture, building and construction: guidelines for corrosion prevention, Nickel development institute (2001)

³⁰ T.L. Sudesh, L. Wijesinghe, D.J. Blackwood, "Real time pit initiation studies on stainless steels: the effect of sulphide inclusions", *Corrosion Science*. 49 (2007) 1755–1764.

³¹ A. Pardo et al., "Pitting corrosion behaviour of austenitic stainless steels – combining effects of Mn and Mo additions", *Corrosion Science* 50 (2008) 1796–1806

³² F.P. Ijsseling, *Survey of Literature on Crevice Corrosion 1979-1998*, Institute of Materials (2001)

³³ Llewellyn, D. T., *Steels: Metallurgy and Applications*, Butterworth-Heinemann, (1992)

³⁴ S. Azuma et al., "Effect of nickel alloying on crevice corrosion resistance of stainless steels", *Corrosion Science* 46 (2004) 2265–2280

³⁵ Schütze, M. ed., *Corrosion and Environmental Degradation*, Wiley-Vch Weinheim, (2000)

³⁶ Roger Francis, *Galvanic Corrosion: A Practical Guide to Engineers*, NACE International: The Corrosion Society, (2001)

-
- ³⁷ K. Fushimi et al., "Current distribution during galvanic corrosion of carbon steel welded with type-309 stainless steel in NaCl solution", *Corrosion Science* 50 (2008) 903-911
- ³⁸ Gooch, T. G., *Weld decay in austenitic stainless steel*, The Welding Institute, Cambridge, (1975)
- ³⁹ Valdimir Cihal, *Intergranular Corrosion of Steels and Alloys*, Elsevier Science, (1984)
- ⁴⁰ M. Terada et al., "Investigation on the intergranular corrosion resistance of the AISI 316L(N) stainless steel after long time creep testing at 600 °C", *Materials Characterization* 59 (2008) 663-668
- ⁴¹ R. Roberge, "The Analysis of Spontaneous Electrochemical Noise for Corrosion Studies", *Journal of Applied Electrochemistry* 23 (1993) 1223-1231
- ⁴² T. Anita, M.G. Pujar, H. Shaikh, et al., "Assessment of stress corrosion crack initiation and propagation in AISI type 316 stainless steel by electrochemical noise technique", *Corrosion Science* 48 (2006) 2689-2710
- ⁴³ R. Gibala and R. Hehemann, *Hydrogen Embrittlement and Stress Corrosion Cracking* by , ASM International, first edition, (1984)

⁴⁴ M.I. Suleiman, R.C. Newman, "Crevice stress corrosion test for austenitic stainless steels in hot chloride solutions", *Corrosion* 51 (1995) 171-176

⁴⁵ Y.Y. Chen, Y.M. Liou, H.C. Shih, "Stress corrosion cracking of type 321 stainless steels in simulated petrochemical process environments containing hydrogen sulfide and chloride", *Materials Science and Engineering A* 407 (2005) 114-126

⁴⁶ Muraleedharan, J.B. Gnanamoorthy, P. Rodriguez, "The effect of ageing at 973K on stress corrosion cracking of Type 304 stainless steel", *Corrosion Science* 38 (1996) 1187-1201

⁴⁷ ASTM G 36, Annual Book of ASTM Standards, vol. 03.02, ASTM International, West Conshohocken, PA, 2000. "Evaluating Stress Corrosion Cracking Resistance of Metals and Alloys in Boiling Magnesium Chloride Solution"

⁴⁸ ASTM G 30-97, Annual Book of ASTM Standards, vol. 03.02, ASTM International, West Conshohocken, PA, 2003. "Making and Using U-Bend Stress-Corrosion Test Specimens"

⁴⁹ ASTM G 1-03, Annual Book of ASTM Standards, vol. 03.02, ASTM International, West Conshohocken, PA, 2003. "Preparing, Cleaning, and Evaluating Corrosion Test Specimen"

1918

...

...

...

...

...

...

...

...

1914

MEMORANDUM

114

1. The following information was obtained from the records of the Department of the Interior, Bureau of Land Management, on the subject of the land in question.

2. The land in question is situated in the County of ... State of ... and is owned by ...

3. The land in question is situated in the County of ... State of ... and is owned by ...

4. The land in question is situated in the County of ... State of ... and is owned by ...

5. The land in question is situated in the County of ... State of ... and is owned by ...

(ASTM G36)، فإن كلوريدات الماغنيسيوم – عند درجة الغليان – توفر البيئة المناسبة لتسريع التآكل الإجهادي . و أجريت التجارب على عينات مختلفة مصنعة على شكل الحرف اللاتيني (U)، و ذلك لأن هذا الشكل يحتوي على أنواع مختلفة من الاجهادات التشكيلية و المرنة. و تم تسجيل الوقت اللازم لبداية ظهور الشقوق في جميع العينات. و بعد ذلك تم فحص العينات بواسطة مجهر المسح الإلكتروني.

أظهرت النتائج المخبرية أن التآكل هو من نوع التآكل الإجهادي و ذلك بسبب وجود الكلوريدات و كبريتيد الهيدروجين و الماء في درجات حرارة مرتفعة نسبيا. كما بينت النتائج أن سبائك مادة النيكل Inconel أظهرت مقاومة أفضل للتآكل الإجهادي مقارنة بالفولاذ الغير قابل للصدأ من نوع 316L ، حيث استغرق ظهور الشقوق في سبائك مادة النيكل Inconel 56 يوما مقارنة ب 24 يوما في مادة الفولاذ الغير قابل للصدأ من نوع 316L . و أظهرت صور مجهر المسح الإلكتروني للعينات بأن الشقوق في الفولاذ الغير قابل للصدأ من نوع 316L أطول و أعرض و أعمق من تلك التي ظهرت في عينات سبائك مادة النيكل Inconel.

UAEU LIBRARY



1000456950

مكتبات الطالبات بالمقام
MAQAM LIBRARIES



ملخص البحث

تعتبر دولة الإمارات العربية المتحدة من الدول الرئيسية المنتجة للنفط والغاز الطبيعي وتشكل عائدات تصدير النفط حوالي 30 في المئة من الناتج المحلي الاجمالي. كما تشكل احتياطات الدولة 10 في المئة من اجمالي احتياطات العالم كافة من النفط الخام.

سجلت إحدى منشآت تصنيع الغاز الطبيعي في مدينة أبوظبي، حالتين لتهالك المواد في الأجزاء الداخلية لأبراج تقطير المكثفات البترولية ، و ذلك خلال عامين، و حيث أن المادة المستخدمة لتصنيع الأجزاء الداخلية لأبراج التثبيت كانت من الفولاذ الغير قابل للصدأ من نوع 316L تم في هذا البحث دراسة أنواع متعددة من تآكل الفولاذ الغير قابل للصدأ، مع التركيز على الشقوق الناتجة عن التآكل الإجهادي ، بالإضافة إلى دراسة خواص السبائك فائقة الجودة و خاصة سبائك مادة النيكل.

لقد تم بحث تهالك المواد في أبراج التقطير مع الأخذ بالاعتبار جميع العوامل المؤثرة من ظروف تشغيلية و أنواع التهالك. فأجريت عدة تجارب لتحليل مغذيات البرج و منتجاته. هذا بالإضافة إلى التجارب التي أجريت لتحديد وجود الكلوريدات في المناطق الأكثر تعرضاً للتآكل.

و سعياً لإجراء تجارب التآكل الإجهادي في بيئة مسرّعة، تم إجراء التجارب وفق معايير المعهد الأمريكي للتجارب و المواد (ASTM). و على الرغم من أن هذه المعايير لا تطابق الظروف التشغيلية تماماً، إلا إنها ترشدنا إلى المواد الأكثر مقاومة للتآكل الإجهادي.

وقد اشتملت التجارب العملية اختبارات على الفولاذ الغير قابل للصدأ من نوع 316L في بيئة مسرّعة للتآكل الإجهادي. و تم مقارنة نتائجها مع نتائج اختبارات سبائك النيكل فائقة الجودة من نوع Inconel . وفقاً لمعيار





جامعة الإمارات العربية المتحدة
عمادة الدراسات العليا
برنامج علوم و هندسة المواد

محاكاة تأكل الفولاذ المقاوم للصدأ من نوع
(316L)

في أبراج تقطير المكثفات البترولية لاختيار المواد الأنسب
إعداد

عفيف سيف ناصر هرره

أطروحة مقدمة لعمادة الدراسات العليا ضمن متطلبات الحصول على درجة
الماجستير في علوم و هندسة المواد

إشراف

الدكتور/ سعود الدعجه

الدكتور/ أحمد العور

قسم الهندسة الميكانيكية
كلية الهندسة

نوفمبر 2008